

2

NPS-ME-93-006

NAVAL POSTGRADUATE SCHOOL Monterey, California

AD-A273 879



DTIC
ELECTE
DEC 17 1993
S E D

**EFFECT OF INITIAL IMPERFECTIONS ON THE
RESPONSE OF CYLINDERS TO UNDERWATER
SHOCK**

by

**LT D. T. Hooker, USN
Professor Y. S. Shin, Principal Investigator
Professor Y. W. Kwon, Co-Investigator**

October 1, 1992 - September 30, 1993

Approved for public release; distribution is unlimited.

Prepared for: Defense Nuclear Agency
Alexandria, VA 20311

Naval Postgraduate School
Monterey, CA 93943

93 12 16 021

93-30530



**Best
Available
Copy**

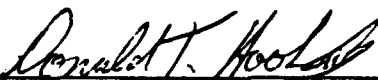
Naval Postgraduate School
Monterey, California

Rear Admiral T. A. Mercer
Superintendent

H. Shull
Provost

This report was prepared for and funded by both the Defense Nuclear Agency, Alexandria, VA 20311 and the Naval Postgraduate School, Monterey, CA 93943.

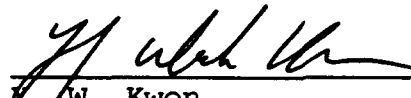
This report was prepared by:



D. T. Hooker II
LT, USN



Y. S. Shin
Professor of Mechanical Engineering



Y. W. Kwon
Associate Professor of Mechanical Engineering

Reviewed by:

Released by:



M. D. Kelleher
Chairman
Dept. of Mechanical Engineering



P. J. Marto
Dean of Research

REPORT DOCUMENTATION PAGE

Form Approved OMB No. 0704

Public reporting burden for this collection of information is estimated to average 1 hour per response, including the time for reviewing instruction, searching existing data sources, gathering and maintaining the data needed, and completing and reviewing the collection of information. Send comments regarding this burden estimate or any other aspect of this collection of information, including suggestions for reducing this burden, to Washington headquarters Services, Directorate for Information Operations and Reports, 1215 Jefferson Davis Highway, Suite 1204, Arlington, VA 22202-4302, and to the Office of Management and Budget, Paperwork Reduction Project (0704-0188) Washington DC 20503.

1. AGENCY USE ONLY		2. REPORT DATE 30 September 1993	3. REPORT TYPE AND DATES COVERED DNA Progress Report 10/92 to 9/93	
4. TITLE AND SUBTITLE EFFECT OF INITIAL IMPERFECTIONS ON THE RESPONSE OF CYLINDERS TO UNDERWATER SHOCK			5. FUNDING NUMBERS	
6. AUTHOR(S) <i>D. T. Hooker, Y. S. Shin and Y. W. Kwon</i>				
7. PERFORMING ORGANIZATION NAME(S) AND ADDRESS(ES) Naval Postgraduate School Monterey, CA 93943-5000			8. PERFORMING ORGANIZATION REPORT NUMBER NPS-ME-93-006	
9. SPONSORING/MONITORING AGENCY NAME(S) AND ADDRESS(ES) Defense Nuclear Agency Alexandria, VA 22310			10. SPONSORING/MONITORING AGENCY REPORT NUMBER	
11. SUPPLEMENTARY NOTES The views expressed in this thesis are those of the authors and do not reflect the official policy or position of the Department of Defense or the U.S. Government.				
12a. DISTRIBUTION/AVAILABILITY STATEMENT Approved for public release; distribution is unlimited.			12b. DISTRIBUTION CODE *A	
13. ABSTRACT Presently, the United States Navy is searching for an improved method to predict the damage to a ship or underwater structure that results from an underwater explosion. One method of predicting this damage is through the use of nonlinear finite and boundary element analysis. Underwater Shock Analysis (USA) combined with VEC/DYNA3D is used for the analysis of the effect of explosive shock on numerical models. Initial imperfections are introduced in the numerical model using modal imperfections. The resulting numerical model is then subjected to a simulated underwater shock using the combined USA/DYNA3d code. A sensitivity analysis is performed to look into the details on the damage resulting from these simulations.				
14. SUBJECT TERMS UNDERWATER SHOCK, INITIAL IMPERFECTIONS			15. NUMBER OF PAGES 72	
			16. PRICE CODE	
17. SECURITY CLASSIFICATION OF REPORT Unclassified	18. SECURITY CLASSIFICATION OF THIS PAGE Unclassified	19. SECURITY CLASSIFICATION OF ABSTRACT Unclassified	20. LIMITATION OF ABSTRACT UN	

NSN 7540-01-280-5500

Standard Form 298 (Rev. 2-89)
Prescribed by ANSI STD. Z39-18

ABSTRACT

Presently, the United States Navy is searching for an improved method to predict the damage to a ship hull or underwater structure that results from an underwater explosion. One method of predicting this damage is through the use of nonlinear finite and boundary element analysis. Underwater Shock Analysis (USA) combined with VEC/DYNA3D is used for the analysis of the effect of explosive shock on numerical models. Initial imperfections are introduced in the numerical model using modal imperfections. The resulting numerical model is then subjected to a simulated underwater shock using the combined USA/DYNA3D code. A sensitivity analysis is performed to look into the details on the damage resulting from these simulations.

Accession For	
NTIS CRA&I	<input checked="" type="checkbox"/>
DTIC TAB	<input type="checkbox"/>
Unannounced	<input type="checkbox"/>
Justification	
By	
Distribution /	
Availability Codes	
Dist	Avail and/or Special
A-1	

DTIC QUALITY INSPECTED 1

TABLE OF CONTENTS

I.	INTRODUCTION	1
II.	INITIAL IMPERFECTIONS	2
III.	TWO DIMENSIONAL INFINITE CYLINDER MODELS	5
	A. Perfect Cylinder Model	7
	B. Imperfect Cylinder Models10
IV.	THREE DIMENSIONAL RING STIFFENED INFINITE CYLINDER MODELS15
	A. Perfect Cylinder Models15
	B. Imperfect Cylinder Models18
V.	THREE DIMENSIONAL RING STIFFENED FINITE LENGTH CYLINDER26
	A. Perfect Cylinder Models26
	B. Imperfect Cylinder Models28
	C. Exponential Decay Shock Wave46
VI.	SUMMARY AND CONCLUSIONS56
	REFERENCES58
	APPENDIX A: INGRID INPUT FILE FOR TWO DIMENSIONAL INFINITE CYLINDER MODEL59
	APPENDIX B: INGRID INPUT FILE FOR THREE DIMENSIONAL RING STIFFENED INFINITE CYLINDER MODEL60
	APPENDIX C: INGRID INPUT FILE FOR THREE DIMENSIONAL RING STIFFENED FINITE CYLINDER MODEL62
	APPENDIX D: FORTRAN PROGRAMS FOR MODIFYING INGRIDO FILE FOR MODAL IMPERFECTIONS65
	INITIAL DISTRIBUTION LIST72

I. INTRODUCTION

The use of USA/DYNA3D for analyzing structures subjected to underwater shock has been shown to be an effective tool in predicting the response of these structures and the resulting damage (Chisum 1992). In some cases the actual deformation of a cylinder subjected to an underwater shock is not accurately predicted. One explanation for this inaccuracy is that actual cylinders have many imperfections (e.g., out of roundness, thin sections, voids, etc.) and the finite element modeling of these cylinders often do not take into account the initial imperfections that are present. By introducing imperfections in the position of the node points generated by a finite element mesh generator it is possible to more accurately model the geometry of an actual cylinder. With a more accurate model of the actual cylinder the finite element numerical analysis of the resulting damage due to underwater shock may be more accurate as well.

II. INITIAL IMPERFECTIONS

The location of the node points of a structure modeled by a finite element mesh generator are precisely located (to the numerical accuracy of the modeling code) at the positions specified in the inputs to the mesh generator algorithm. Manufactured structures usually have many imperfections that are not accurately modeled by many finite element mesh generators. Surveys have been performed to measure the imperfections that naturally exist in cylindrical shell structures (Arbocz 1982). These data have been collected into data banks, and Arbocz suggests that they be used to improve design criteria for buckling of thin shells. The imperfection data banks show that imperfections have characteristic distributions that include decreasing modal amplitudes with increasing mode number. Kirkpatrick (1989) found that by introducing initial modal imperfections in a cylindrical structure subjected to blast shock loading that the resulting numerical analysis agreed much closer to the experimental data than the analysis without these initial imperfections.

Initial imperfections were introduced into the location of the node points of the finite element model using a summation of modal imperfections expressed as the cosine series shown in Eq. (1).

$$\Delta R(\theta) = \sum_{n=2}^N A_n \cos(n\theta + \phi_n) \dots \dots \dots (1)$$

where ΔR is the radial imperfection, θ is the angular position, N is the maximum modal contribution, A_n is the modal amplitude, and ϕ_n is a random modal phase shift. The assumption that the modal phase shift is a random variable is reasonable for many shells. An empirical form for the modal amplitude is expressed as shown in Eq. (2).

$$A_n = \frac{X}{n^r} \dots \dots \dots (2)$$

where A_n is the modal amplitude of the n th modal imperfection, n is the mode number and X and r are coefficients used to fit the available data for shells of a given construction. The modal amplitude can be modeled as a constant percentage of the shell thickness. For many of the studies in this investigation the modal amplitude is constant as shown in Eq. (3) at 1% of the shell thickness for all modes.

$$A_n = 0.01h \quad \text{for all } n \dots \dots \dots (3)$$

Kirkpatrick found that the modal amplitudes in Eq. (4) and (5) accurately modeled the imperfections of his test cylinder.

$$A_n = 0.05h \quad n \leq 6 \quad \dots \dots \dots (4)$$

$$A_n = \frac{2h}{n^2} \quad n \geq 7 \quad \dots \dots \dots (5)$$

The modal imperfections introduced in this study are assumed to be a function only of the circumferential position of the node and not a function of the axial position of the node.

III. TWO DIMENSIONAL INFINITE CYLINDER MODELS

Fox (1992) developed a two dimensional infinite cylinder model to validate the use of the USA/DYNA3D code for use in underwater shock analysis. This model was further developed into the full symmetry two dimensional infinite cylinder model shown in Figure 1. This model has 40 elements around the circumference of the cylinder, radius of 6 inches, shell thickness of 0.06 inches and an element length of 0.006 inches. The same restriction on the length of the elements found for the model Fox developed (length/radius=0.001) was also true for this model. Fox stated that longer elements resulted in 'residual three dimensional effects' that caused oscillations in the numerical results. Symmetric boundary conditions were imposed on both ends of the cylinder to model an infinite length cylinder. This model and all subsequent models (unless specifically noted) use Belytschko-Tsay (Belytschko 1984) shell elements for their numerical efficiency and to eliminate the problems of using a solid element to model a thin walled structure. The shell material is modeled as mild steel, an elastic-plastic material with a Young's modulus of 2.9×10^7 psi, a Poisson's ratio of 0.3, a hardening modulus of 5100 psi and a yield stress of 32,000 psi.

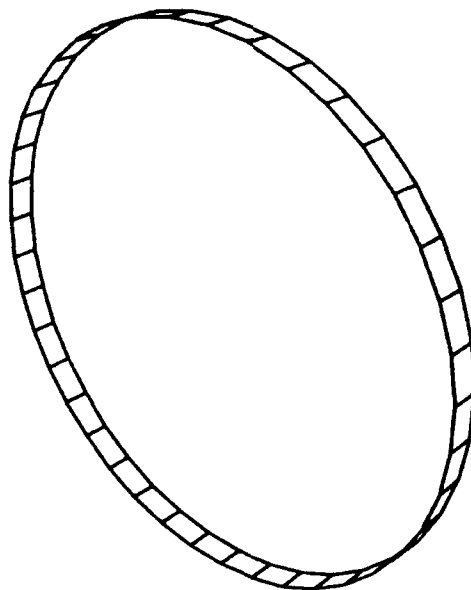
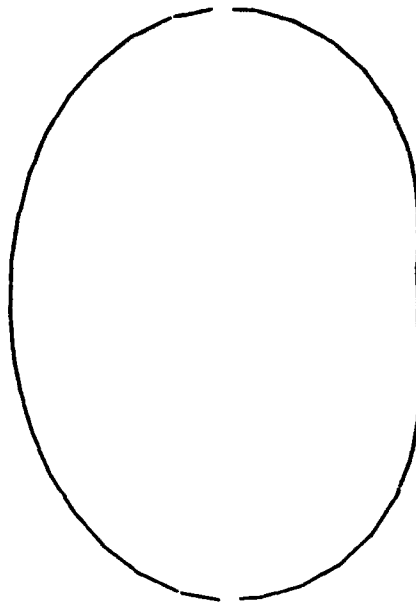


Figure 1. Two Dimensional Infinite Cylinder Model

A. Perfect Cylinder Model

This cylinder was subjected to a underwater shock wave modeled as a plane wave with an amplitude of 500 psi and a duration of 1 millisecond resulting from an explosive charge located along the x-axis. The early damage pattern at 0.5 milliseconds is shown in Figure 2. The front face of the cylinder is flattened by the impacting plane wave approaching from the right. However, Figure 3 shows that the final damage pattern at 5 milliseconds is very different than this early deformation pattern. All plastic deformation has been completed by 5 milliseconds. The side of the cylinder facing the approaching shock wave shows a pronounced protrusion. This pattern was unexpected based on experimental results which have usually shown inward deformations of a cylindrical shell facing the explosive charge. It is hypothesized that this raised section is due to the fact that the modeled cylinder is a perfect cylinder and is not representative of a true manufactured cylinder. The manufactured cylinder will have many imperfections in the shell which is not present in the computer models.

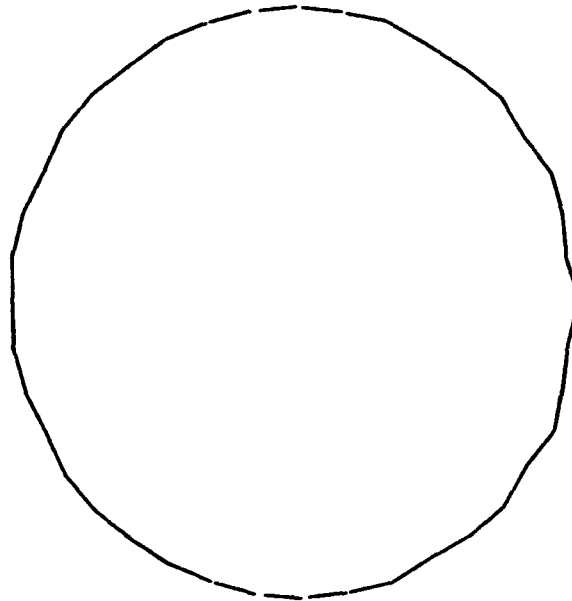
In order to study the effect of mesh size on the response of this cylinder another model was developed with 64 elements around the circumference of the cylinder. Figure 4 shows that the response of this cylinder is similar to that for the 40 element cylinder. There is still a



← Shock
Wave

0.5 ms (deformations scaled up 100X)

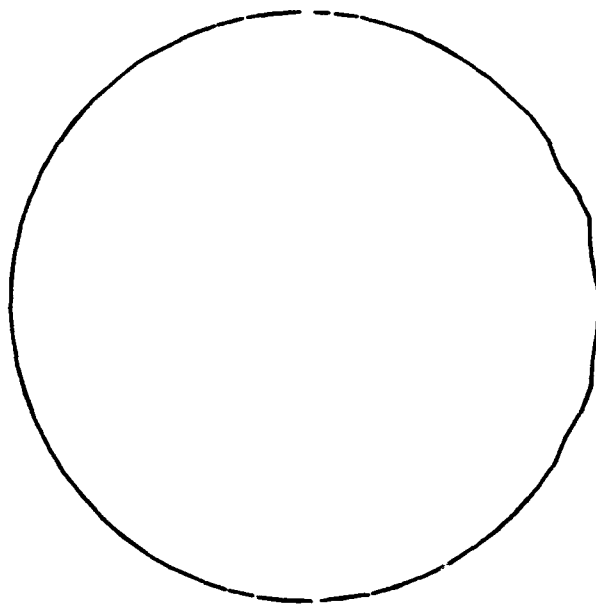
Figure 2. Deformation of Two Dimensional Infinite Cylinder
Subjected to a Square Pressure Pulse of 500 psi for 1ms



← Shock
Wave

5.0 ms (deformations scaled up 10X)

Figure 3. Deformation of Two Dimensional Infinite Cylinder
Subjected to a Square Pressure Pulse of 500 psi for 1ms



← Shock
Wave

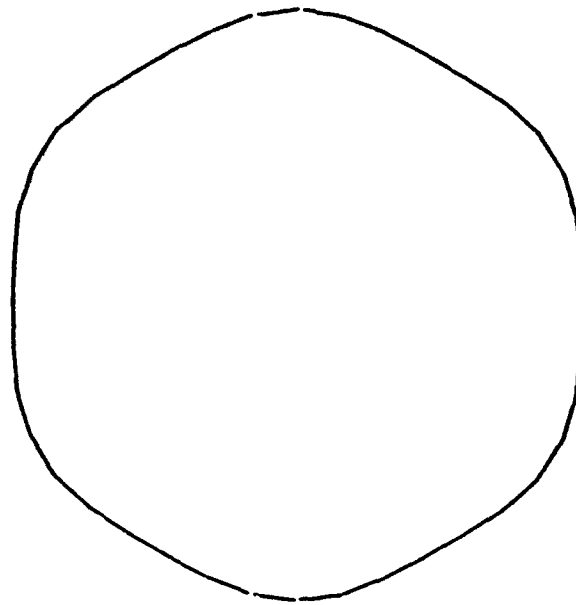
5.0 ms (deformations scaled up 10X)

Figure 4. Deformation of Two Dimensional Infinite Cylinder
Subjected to a Square Pressure Pulse of 500 psi for 1ms
Fine Mesh

distinct protrusion of the shell toward the direction of the approaching shock wave. All subsequent cylinders will use 40 elements around the circumference of the cylinder.

B. Imperfect Cylinder Models

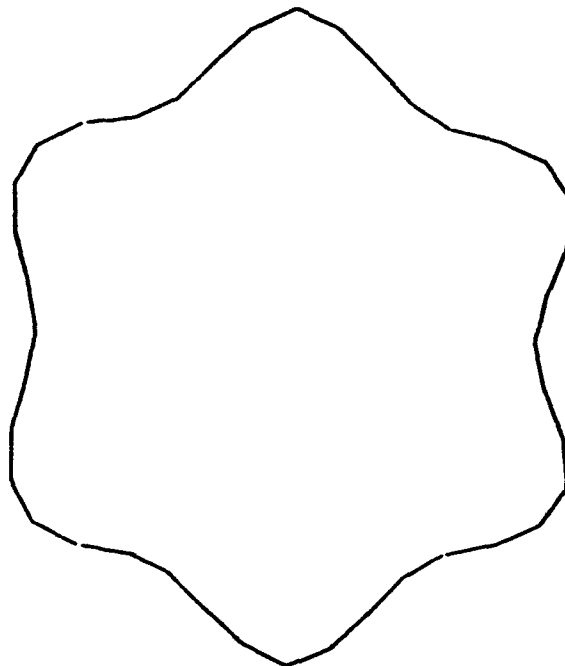
The introduction of initial imperfections significantly changes both the shape and magnitude of the resulting deformation. Introduction of a 6th mode imperfection, as shown in Figure 5 (imperfection magnitude scaled by a factor of 100) with a modal amplitude of 5% of the shell thickness and no random phase shift, results in the damage pattern shown (deformations scaled by factor of 10) in Figure 6. A mode 6 imperfection was chosen because of the ease in identifying its distinctive pattern. Use of another model imperfection would only have changed the shape of the final deformation not any conclusions resulting from this study. Comparison of the final damage pattern with the shape of the initial imperfection shows that the damage pattern follows the initial imperfection resulting in a final damage pattern looking like the mode 6 initial imperfection magnified due to the external shock wave applied to the cylinder. The introduction of imperfections caused the deformation of the cylindrical shell to follow the initial imperfection pattern of the shell. In addition to changing the damage pattern,



←Shock
Wave

Initial Mode 6 Imperfection (imperfections scaled up 100X)

Figure 5. Two Dimensional Infinite Cylinder Subjected to a Square Pressure Pulse of 500 psi for 1ms Mode 6 Initial Imperfection $A_6=0.05h$



←Shock
Wave

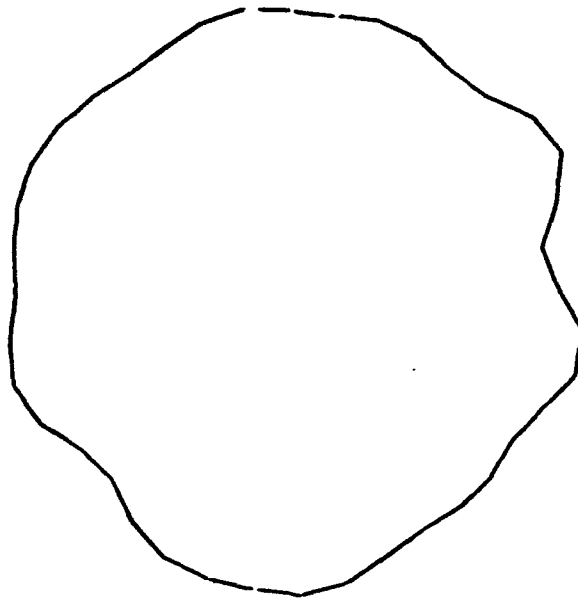
5.0 ms (deformations scaled up 10X)

Figure 6. Two Dimensional Infinite Cylinder Subjected to a Square Pressure Pulse of 500 psi for 1ms Mode 6 Initial Imperfection $A_6=0.05h$

the initial imperfection also causes much greater deflections of the shell for the same shock wave intensity.

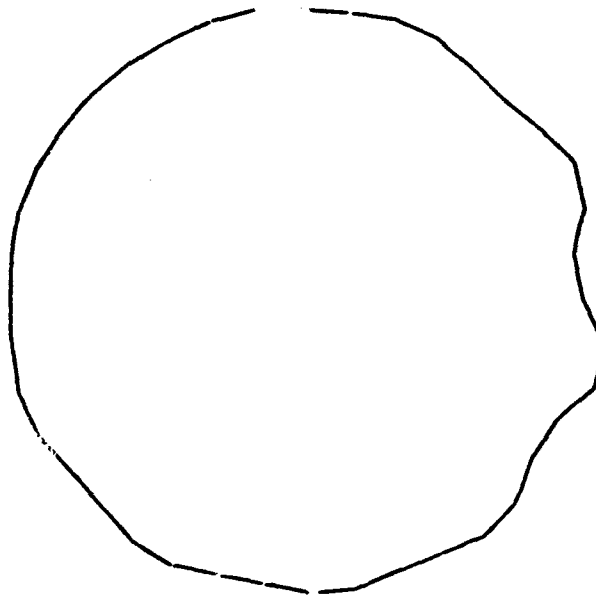
Another cylinder was modeled with imperfections containing the first 10 modal imperfections, as shown in Figure 7 with modal amplitudes for each mode of 1% of the shell thickness and with random phase shifts. The resulting damage pattern is shown in Figure 8. Again, the general shape of the final deformation pattern is very close to the shape of the initial imperfection pattern.

The introduction of a different initial imperfection, shown in Figure 9 with initial imperfections magnified by 50 times, using the modal amplitude of equations (4) and (5), results in the final deformation pattern shown in Figure 10. Again, the deformation of the shell of the cylinder follows the initial imperfection pattern.



Initial Imperfection (imperfections scaled up 200X)

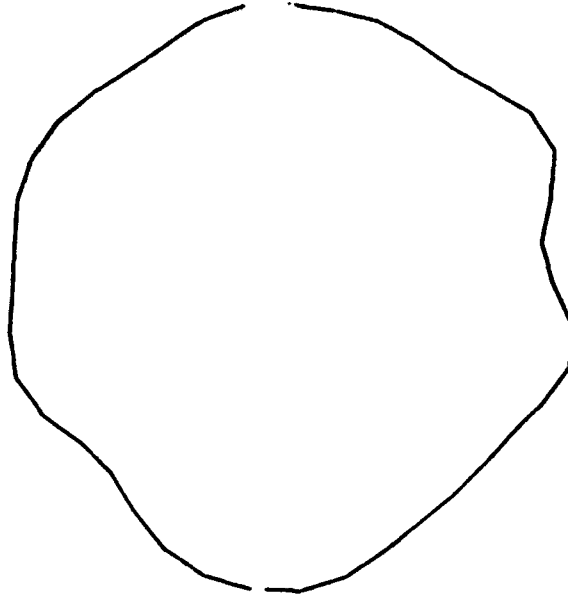
Figure 7. Two Dimensional Infinite Cylinder Subjected to a Square Pressure Pulse of 500 psi for 1ms Initial Imperfection First 10 Modes $A_n=0.01h$ with Random Phase Shift



←Shock
Wave

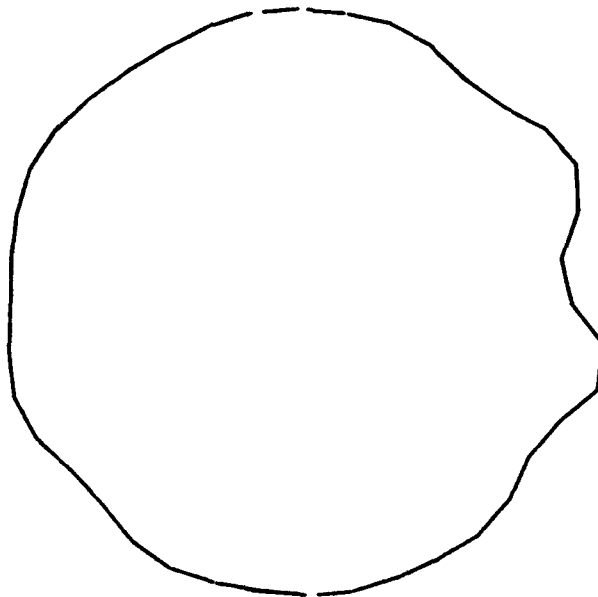
5.0 ms (deformations scaled up 2X)

Figure 8. Two Dimensional Infinite Cylinder Subjected to a Square Pressure Pulse of 500 psi for 1ms Initial Imperfection First 10 Modes $A_n=0.01h$ with Random Phase Shift



Initial Imperfection (imperfections scaled up 50X)

Figure 9. Two Dimensional Infinite Cylinder Subjected to a Square Pressure Pulse of 500 psi 1ms Initial Imperfection First 10 modes $A_n=0.05h$ for Modes 2 through 6, $A_n=2h/n^2$ for Modes 7 through 10



← Shock Wave

5.0 ms (deformations scaled up 2X)

Figure 10. Two Dimensional Infinite Cylinder Subjected to a Square Pressure Pulse of 500 psi 1ms Initial Imperfection First 10 modes $A_n=0.05h$ for Modes 2 through 6, $A_n=2h/n^2$ for Modes 7 through 10

IV. THREE DIMENSIONAL RING STIFFENED INFINITE CYLINDER

MODELS

The three-dimensional ring stiffened infinite cylinder model shown in Figure 11 was developed from the two-dimensional infinite cylinder model. This model has a total of 400 elements with 40 elements in the circumferential direction and 10 elements along the length. Again symmetric boundary conditions were imposed on both ends of the cylinder to model an infinite cylinder. This three-dimensional model has stiffeners 0.12 inches thick and 1 inch deep located on 12 inch spacing. The shell is 0.06 inches thick. The shell and stiffeners are modeled as mild steel with the same properties as listed earlier

A. Perfect Cylinder Model

This cylinder was subjected to the same plane shock wave as the previous models. The early deformation of the cylinder at 0.2 milliseconds (Figure 12) shows the outer shell pinching in on either side of the stiffener located in the center of the cylinder. Figure 13 shows the flattening of the face of the cylinder facing the explosive charge at 0.2 milliseconds. At this time in the deformation history there is no evidence of the formation of a local raised area on the front of the cylinder facing the charge. The final

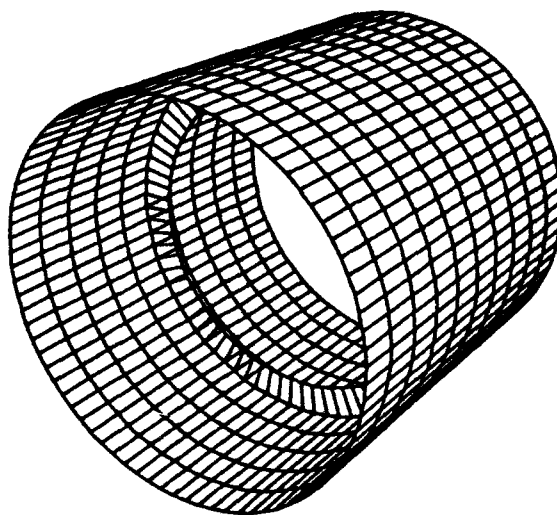
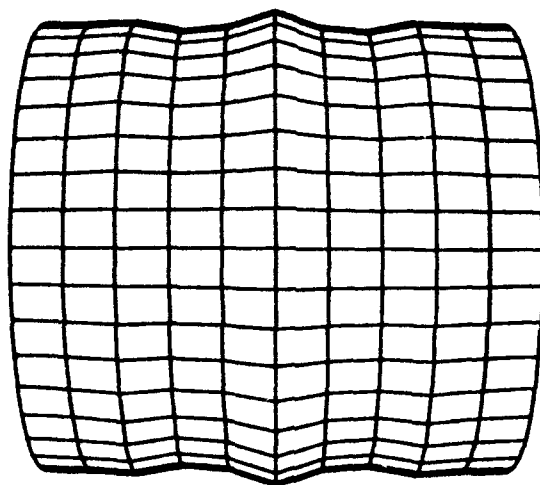
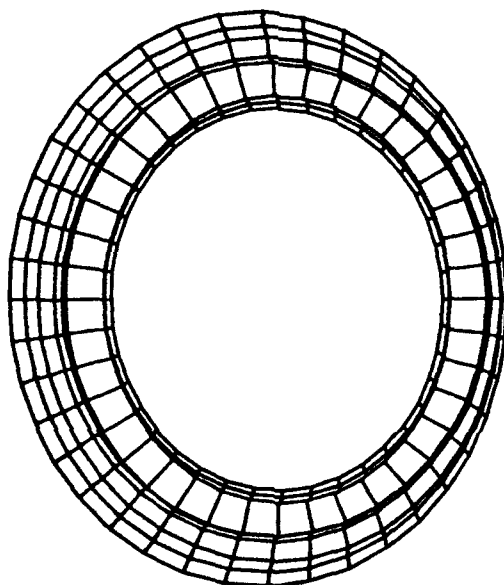


Figure 11. Three Dimensional Ring Stiffened Infinite Cylinder Model



Front View @ 0.2 ms (deformations scaled up 50X)

Figure 12. Deformation of Three Dimensional Ring Stiffened Infinite Length Cylinder Subjected to a Square Pressure Pulse of 500 psi for 1ms



← Shock Wave

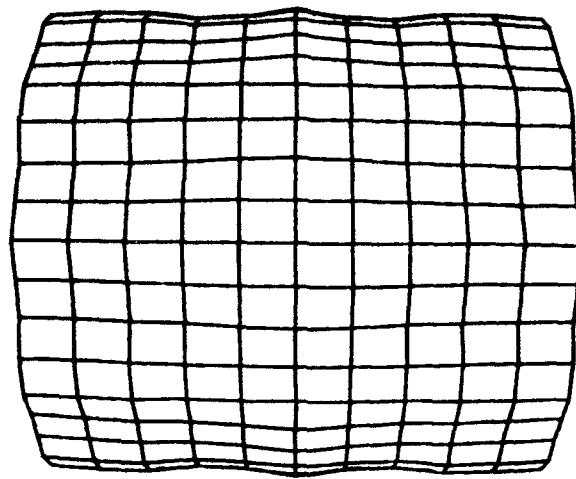
End View @ 0.2 ms (deformations scale up 50X)

Figure 13. Deformation of Three Dimensional Ring Stiffened Infinite Length Cylinder Subjected to a Square Pressure Pulse of 500 psi for 1ms

deformation pattern shown in Figure 14 shows pinching of the shell on either side of the stiffener. This pinching effect was also noted by Chisum (1992) and appears to be present in many finite element simulations of underwater shock which model test cylinders as perfect cylinders. Again, the final deformation pattern of the cylinder side facing the charge has a local protrusion of the shell material toward the explosive charge as shown in Figure 15. Again, it is hypothesized that this damage pattern is the result of the model cylinder being a perfect cylinder while test cylinders will always have imperfections in the shell of the cylinder.

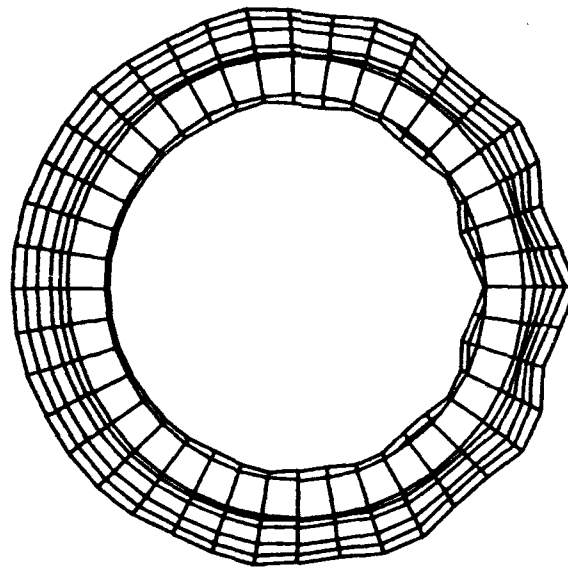
B. Imperfect Cylinder Models

The introduction of initial imperfections significantly changes both the shape and magnitude of the final deformations seen in this cylinder model. The 5% mode 6 imperfection shown in Figure 16 was introduced into this model. The resulting deformation due to a 500 psi 1 millisecond plane wave pressure pulse is shown in Figures 17 through 20. The initial imperfection shape is clearly evident in the final damage pattern. However the shape of the cylinder at 0.2 milliseconds does not show any of the initial imperfection. There is insufficient time elapsed for the deformations to grow large enough to show this initial imperfection. However the pinching of the shell on



Front View @ 5.0 ms

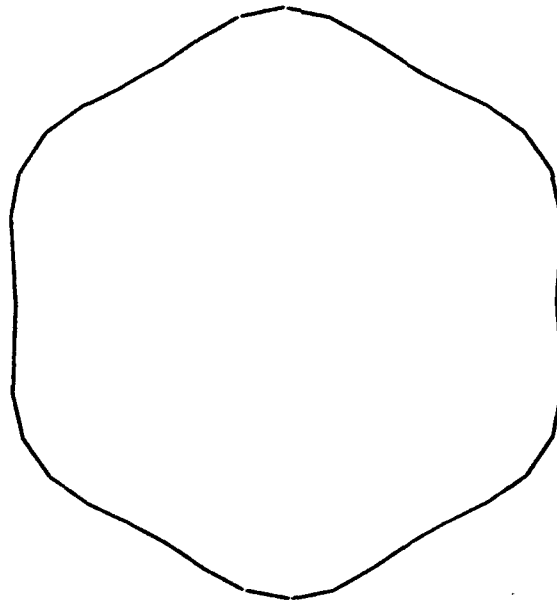
Figure 14. Deformation of Three Dimensional Ring Stiffened Infinite Length Cylinder Subjected to a Square Pressure Pulse of 500 psi for 1ms



← Shock Wave

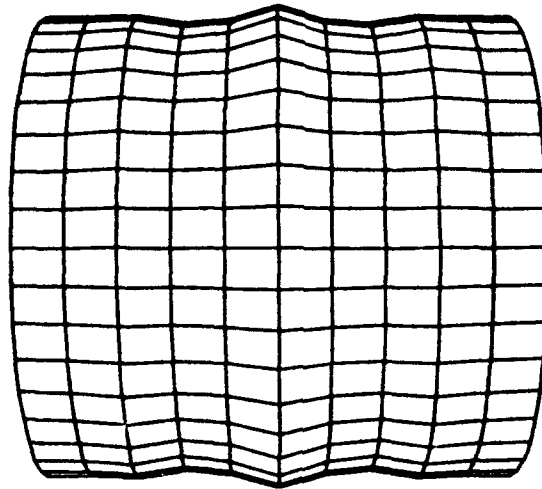
End View

Figure 15. Deformation of Three Dimensional Ring Stiffened Infinite Length Cylinder Subjected to a Square Pressure Pulse of 500 psi for 1ms



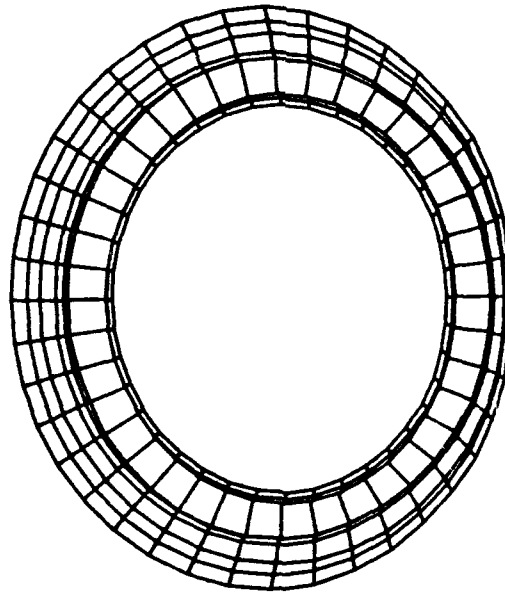
Mode 6 Initial Imperfection $A_6=0.05h$ (imperfections scaled
up 100X)

Figure 16. Deformation of Three Dimensional Ring Stiffened
Infinite Length Cylinder Subjected to a Square Pressure
Pulse of 500 psi for 1ms



Front View @ 0.2 ms (deformations scaled up 50X)

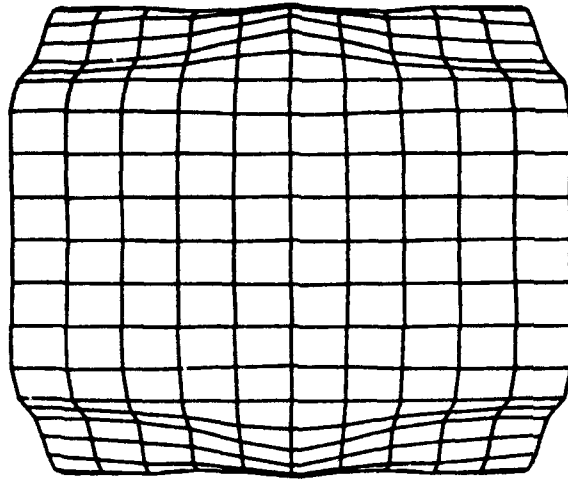
Figure 17. Deformation of Three Dimensional Ring Stiffened Infinite Length Cylinder with a Mode 6 Initial Imperfection $A_6=0.05h$ Subjected to a Square Pressure Pulse of 500 psi for 1ms



← Shock Wave

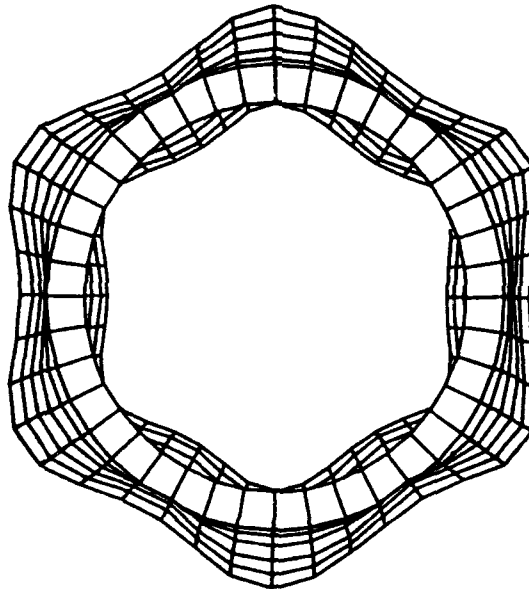
End View @ 0.2 ms (deformations scaled up 50X)

Figure 18. Deformation of Three Dimensional Ring Stiffened Infinite Length Cylinder with a Mode 6 Initial Imperfection $A_6=0.05h$ Subjected to a Square Pressure Pulse of 500 psi for 1ms



Front View @ 5.0 ms

Figure 19. Deformation of Three Dimensional Ring Stiffened Infinite Length Cylinder with a Mode 6 Initial Imperfection $A_6=0.05h$ Subjected to a Square Pressure Pulse of 500 psi for 1ms



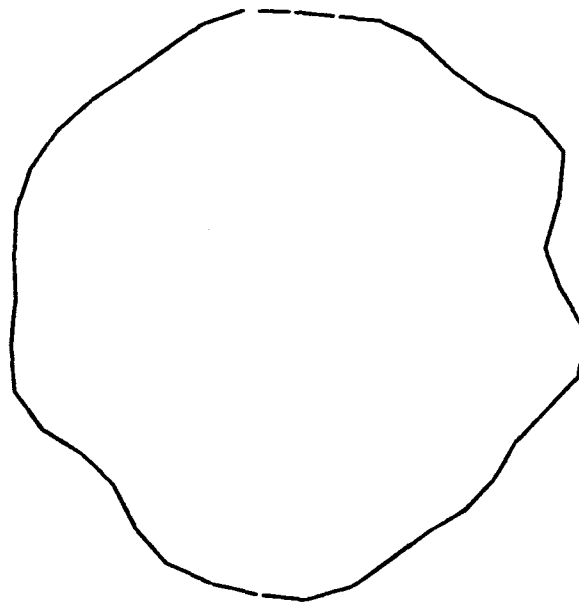
← Shock Wave

End View @ 5.0 ms

Figure 20. Deformation of Three Dimensional Ring Stiffened Infinite Length Cylinder with a Mode 6 Initial Imperfection $A_6=0.05h$ Subjected to a Square Pressure Pulse of 500 psi for 1ms

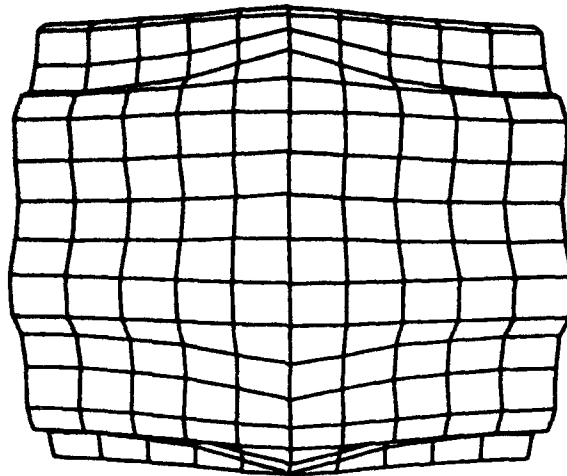
either side of the stiffener has already begun at 0.2 milliseconds. The final deformation still shows this pinching effect however the magnitude of this type of deformation is reduced by the initial imperfection.

With the introduction of an initial imperfection of the first 10 modes with modal amplitudes of 1% of the shell thickness and with random phase shifts as shown in Figure 21 the resulting damage pattern again shows that the deformation of the shell will preferentially follow the initial imperfections. The resulting damage pattern is very different from the perfect case (Figures 22 and 23). Most noteworthy is the elimination of the pinch in the outer shell on either side of the stiffener. In addition the magnitude of the deformation in the outer shell is much greater than for the perfect cylinder case. The introduction of these imperfections results in sites where the cylinder preferentially deforms during the shock pressure. Thus when the cylinder deforms the deformation follows the initial imperfections resulting in the final shape of the cylinder looking like the initial imperfection shape.



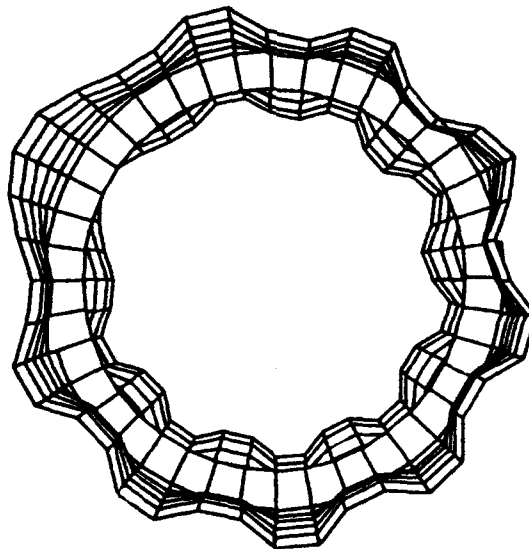
Initial Imperfection (imperfections scaled up 200X)

Figure 21. Three Dimensional Ring Stiffened Infinite Length Cylinder Subjected to a Square Pressure Pulse of 500 psi for 1ms Initial Imperfection First 10 Modes $A_n = 0.01h$ with Random Phase Shift



Front View @ 5.0 ms

Figure 22. Three Dimensional Ring Stiffened Infinite Length Cylinder Subjected to a Square Pressure Pulse of 500 psi for 1ms Initial Imperfection First 10 Modes $A_n=0.01h$ with Random Phase Shift



← Shock Wave

End View @ 5.0 ms

Figure 23. Three Dimensional Ring Stiffened Infinite Length Cylinder Subjected to a Square Pressure Pulse of 500 psi for 1ms Initial Imperfection First 10 Modes $A_n=0.01h$ with Random Phase Shift

V. THREE DIMENSIONAL RING STIFFENED FINITE LENGTH CYLINDER

From the three-dimensional infinite cylinder a three dimensional finite length cylinder was developed as shown in Figure 24. This cylinder is three feet long, 1 foot in diameter with two stiffeners evenly spaced 12 inches apart. The shell of the cylinder is mild steel 0.06 inches thick. The stiffeners are mild steel 0.12 inches thick and 1 inch deep. The endplate is HY-100 steel 0.25 inches thick. The HY-100 steel is modeled as an elastic-plast material with a Young's modulus of 2.9×10^7 psi, a Poisson's ratio of 0.3, a hardening modulus of 5100 psi and a yield stress of 108,000 psi. This cylinder is modeled as a half cylinder with a plane of symmetry perpendicular to the axis of rotation. The model has 40 elements in the circumferential direction and 15 elements in the axial direction for a total of 600 elements and 921 nodes. The use of a half symmetry model with a symmetric boundary condition results in a smaller number of elements and greater computational efficiency for the finite element analysis.

A. Perfect Cylinder Models

This cylinder was subjected to the same planar shock wave as in the previous models. The resulting damage pattern for a perfect cylinder can be seen in Figures 25

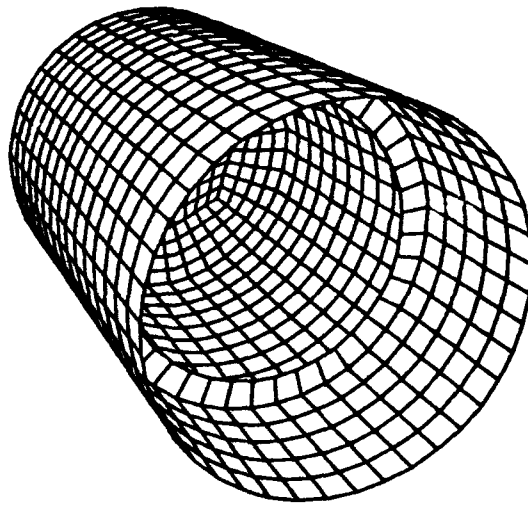


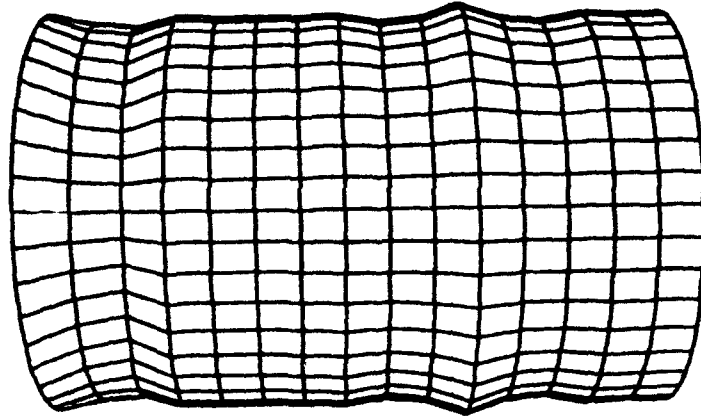
Figure 24

Figure 24. Three Dimensional Ring Stiffened Finite Length Cylinder Model

through 32. Again the side of the cylinder facing the planar shock wave shown a local raised area that was also seen in the previous models. In addition there is a pinch in the shell near the endplates and on either side of the stiffeners. This pinch was also noted by Chisum (1992) during his analysis of DNA models used for underwater shock testing. Most of the deformation of the cylinder shell occurs between 1.0 and 2.0 milliseconds. During the time from 1.0 to 2.0 milliseconds this kinetic energy is transferred to strain energy causing deformation of the shell. After 2.0 milliseconds the most of the plastic deformation has occurred and the cylinder shell then deforms only through elastic vibration. Figure 33 is a plot of the kinetic energy of the cylinder shell as a function of time. The shell has its maximum kinetic energy at 1 ms and then this energy rapidly decreases as it is dissipated into the surrounding medium and into the shell material as strain energy. Figure 34 shows the strain history of the element on the front of the cylinder exactly in the middle of the stiffeners. Again, this plot shows that most of the hoop strain occurs between 1 and 2 milliseconds.

B. Imperfect Cylinder Models

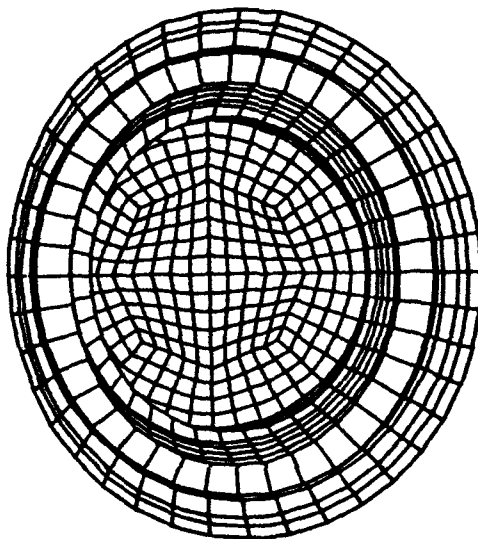
The addition of initial imperfections greatly changes the resulting deformation pattern of the shell of the



Front View @ 0.2 ms (deformations scaled up 50X)

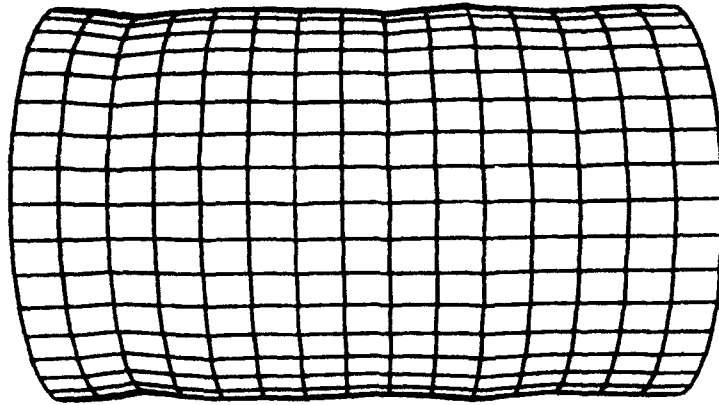
Figure 25. Deformation of Three Dimensional Ring Stiffened Finite Length Cylinder Subjected to a Square Pressure Pulse of 500 psi for 1ms

Shock→
Wave



End View @ 0.2 ms (deformations scaled up 50X)

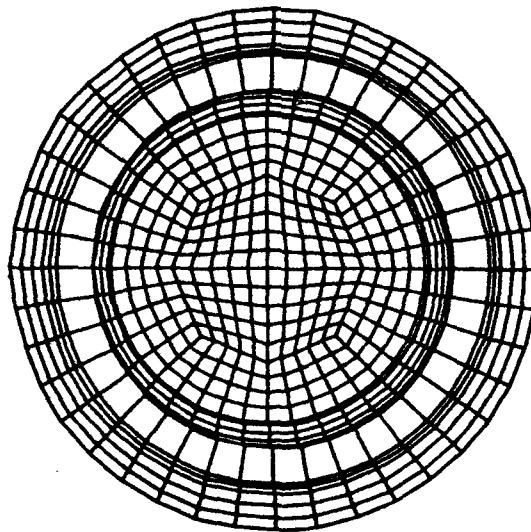
Figure 26. Deformation of Three Dimensional Ring Stiffened Finite Length Cylinder Subjected to a Square Pressure Pulse of 500 psi for 1ms



Front View @ 1.0 ms (deformations scaled up 2X)

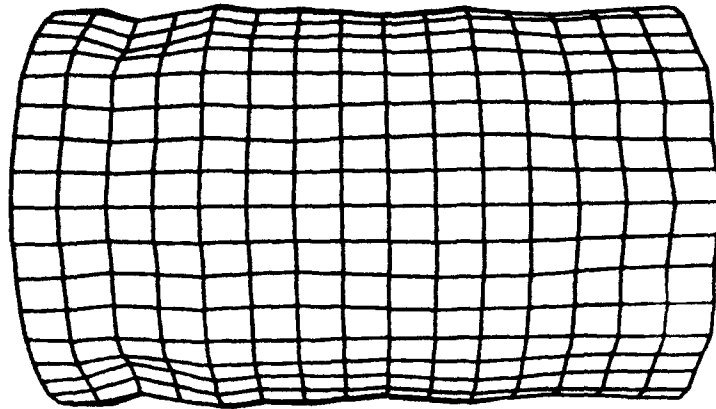
Figure 27. Deformation of Three Dimensional Ring Stiffened Finite Length Cylinder Subjected to a Square Pressure Pulse of 500 psi for 1ms

Shock→
Wave



End View @ 1.0 ms (deformations scaled up 2X)

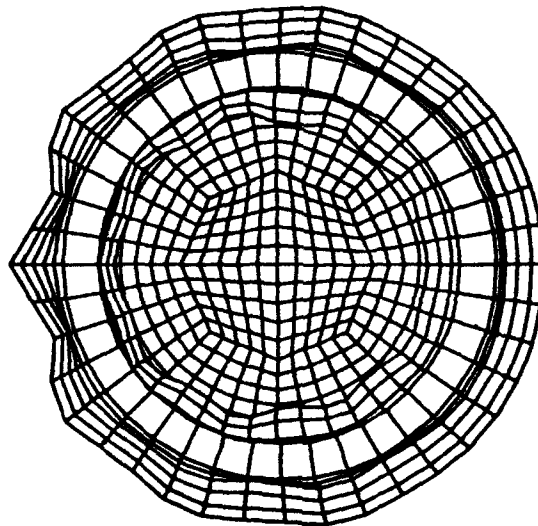
Figure 28. Deformation of Three Dimensional Ring Stiffened Finite Length Cylinder Subjected to a Square Pressure Pulse of 500 psi for 1ms



Front View @ 2.0 ms (deformations scaled up 2X)

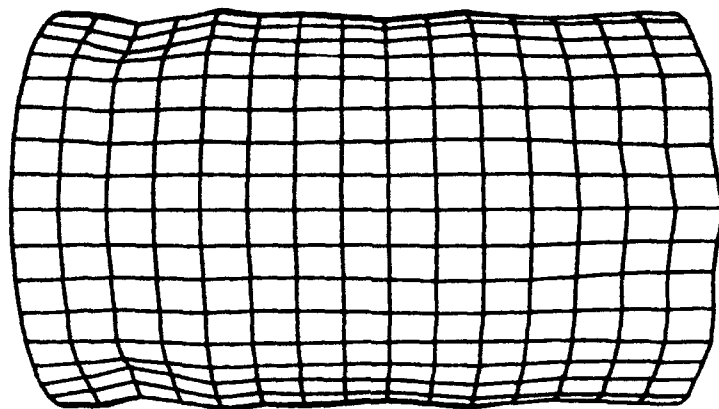
Figure 29. Deformation of Three Dimensional Ring Stiffened Finite Length Cylinder Subjected to a Square Pressure Pulse of 500 psi for 1ms

Shock→
Wave



End View @ 2.0 ms (deformations scaled up 2X)

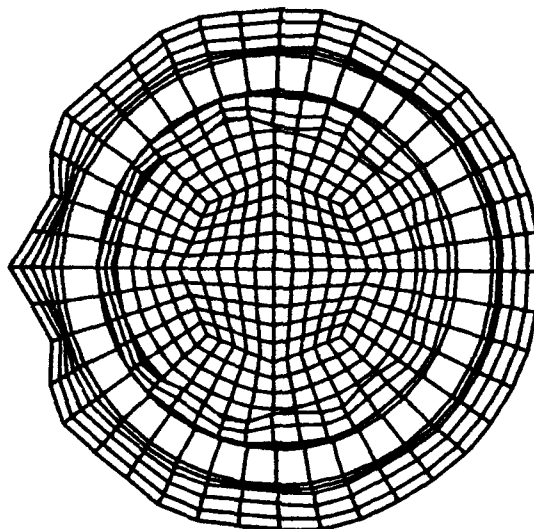
Figure 30. Deformation of Three Dimensional Ring Stiffened Finite Length Cylinder Subjected to a Square Pressure Pulse of 500 psi for 1ms



Front View @ 5.0 ms (deformations scaled up 2X)

Figure 31. Deformation of Three Dimensional Ring Stiffened Finite Length Cylinder Subjected to a Square Pressure Pulse of 500 psi for 1ms

Shock→
Wave



End View @ 5.0 ms (deformations scaled up 2X)

Figure 32. Deformation of Three Dimensional Ring Stiffened Finite Length Cylinder Subjected to a Square Pressure Pulse of 500 psi for 1ms

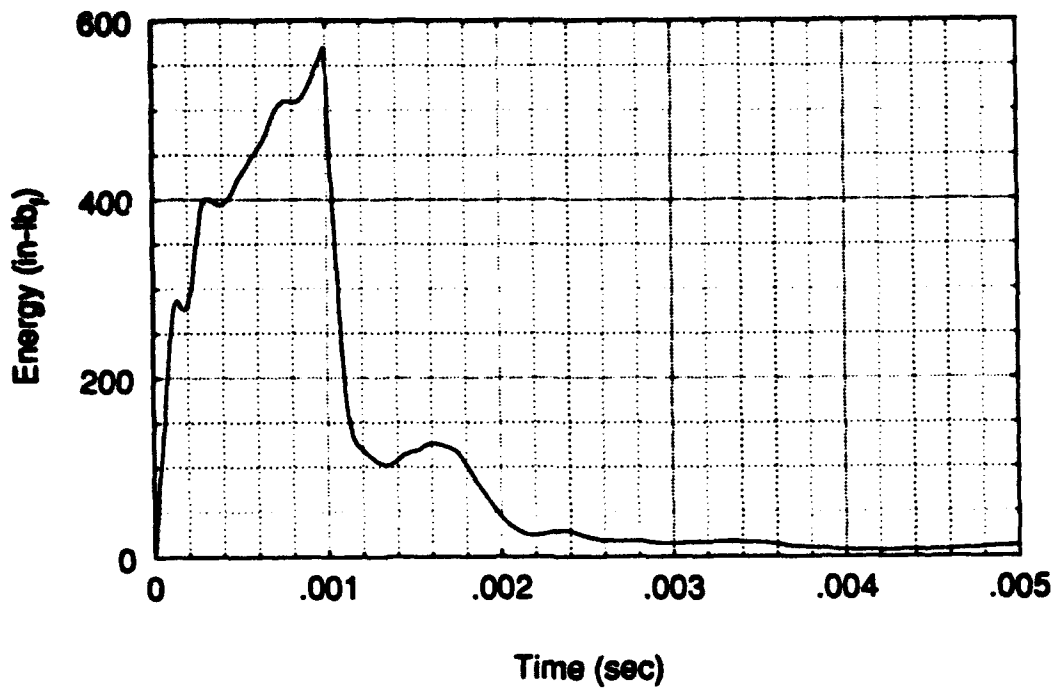


Figure 33. Kinetic Energy of Shell Material

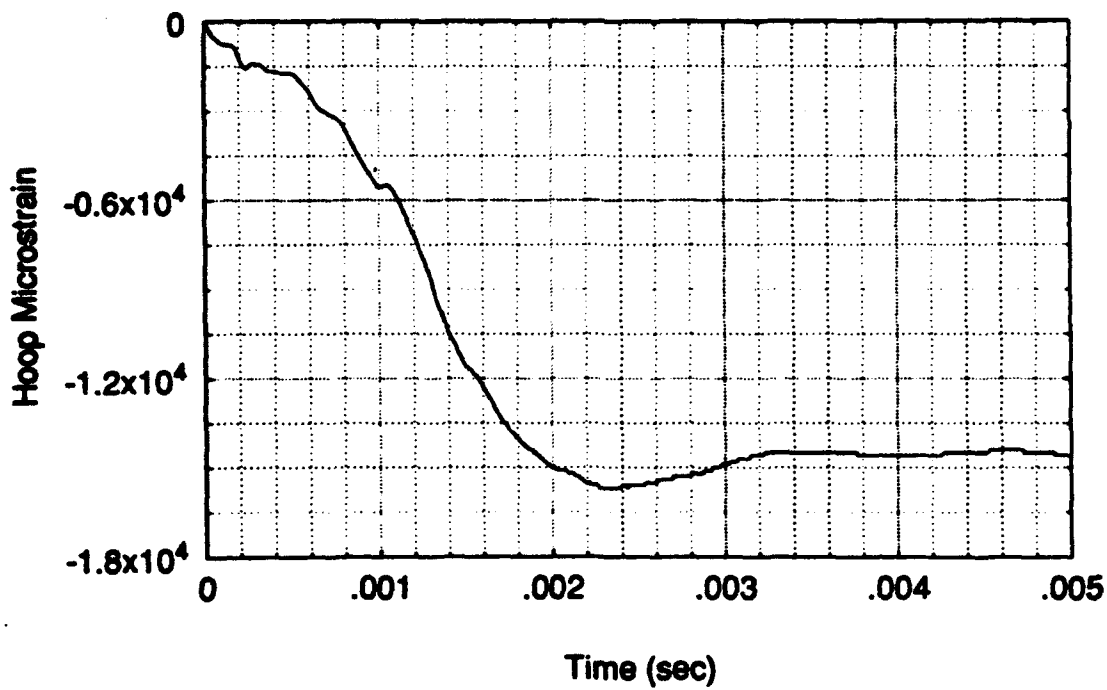
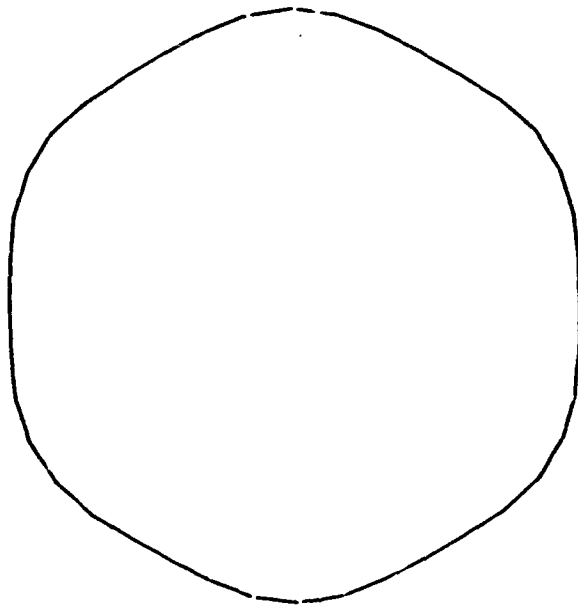


Figure 34. Hoop Strain of Front Middle Element

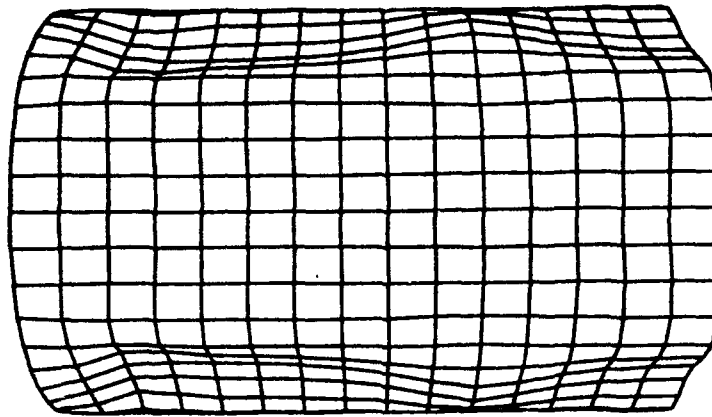
cylinder. The addition of a mode 6 imperfection (shown in Figure 35) with a modal amplitude of 5% of the shell thickness and with no random phase shift results in the final damage pattern shown in Figure 36 and 37. The end view clearly shows the strong effect of the mode 6 initial imperfection causing the final deformation to follow this initial imperfection. The front view of the cylinder shows that the pinching of the shell near the endplates and stiffeners is very much reduced due to the introduction of this imperfection.

An investigation into the effect of the modal amplitude on the final deformation pattern showed that very small modal amplitudes have a significant effect on the response of the cylinder. An initial imperfection consisting of the first 10 mode shapes with varying modal amplitudes and random phase shifts is shown in Figure 38. The resulting damage patterns at various modal amplitudes are shown in Figures 39 through 50. The shell deformation again follows the initial imperfections present in the shell structure. As the modal amplitudes increase the deformation of the shell also increases. At a modal amplitude of 0.01% of the shell thickness the front of the cylinder is distinctly raised toward the explosive charge as in the perfect cylinder. But, it can also be seen from the end view that the deformation pattern even at this magnitude of



Initial Imperfection (imperfections scaled up 100X)

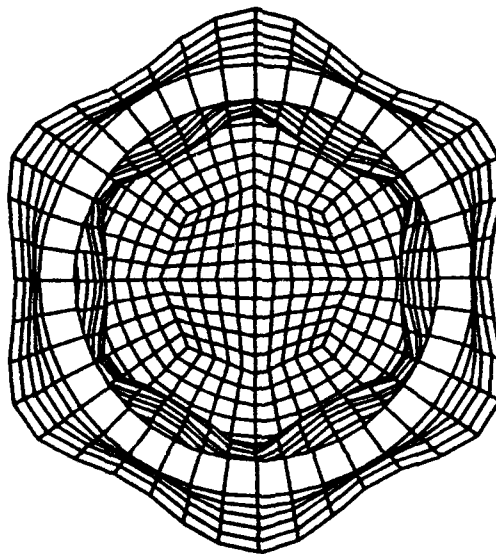
Figure 35. Three Dimensional Ring Stiffened Finite Length
Cylinder Subjected to a Square Pressure Pulse of 500 psi for
1ms Mode 6 Initial Imperfection $A_6=0.05h$



Front View @ 5.0 ms

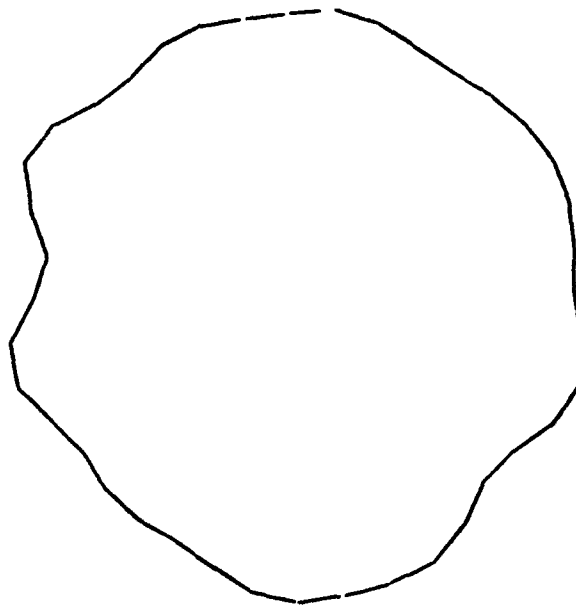
Figure 36. Three Dimensional Ring Stiffened Finite Length Cylinder Subjected to a Square Pressure Pulse of 500 psi for 1ms Mode 6 Initial Imperfection $A_6=0.05h$

Shock→
Wave



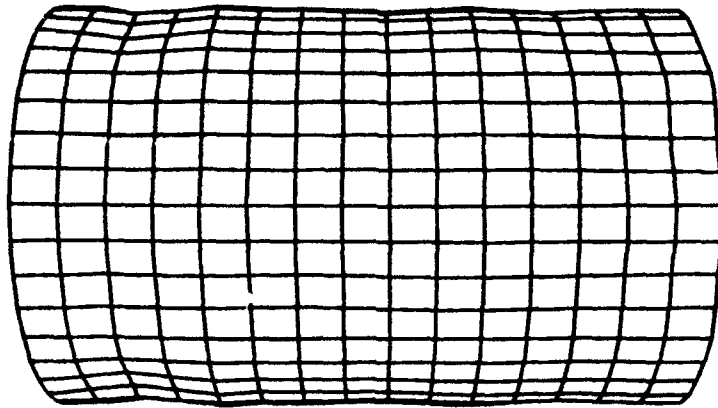
End View @ 5.0 ms

Figure 37. Three Dimensional Ring Stiffened Finite Length Cylinder Subjected to a Square Pressure Pulse of 500 psi for 1ms Mode 6 Initial Imperfection $A_6=0.05h$



Initial Imperfection (imperfections scaled up 200X)

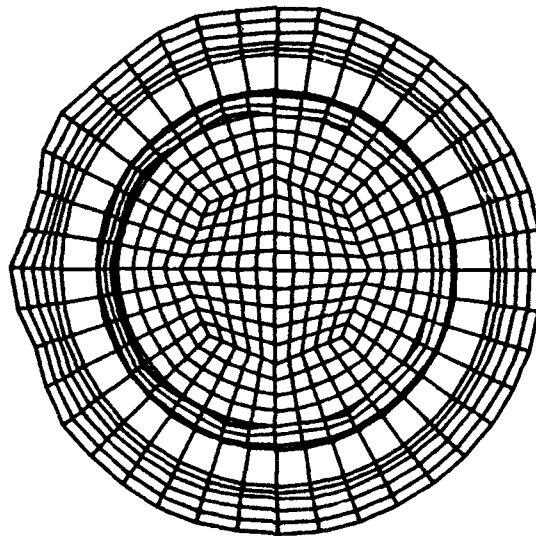
Figure 38. Three Dimensional Ring Stiffened Finite Length
Cylinder Subjected to a Square Pressure Pulse of 500 psi for
1ms First 10 Modes w/Random Phase Shift



Front View $A_s = 0.0001h$

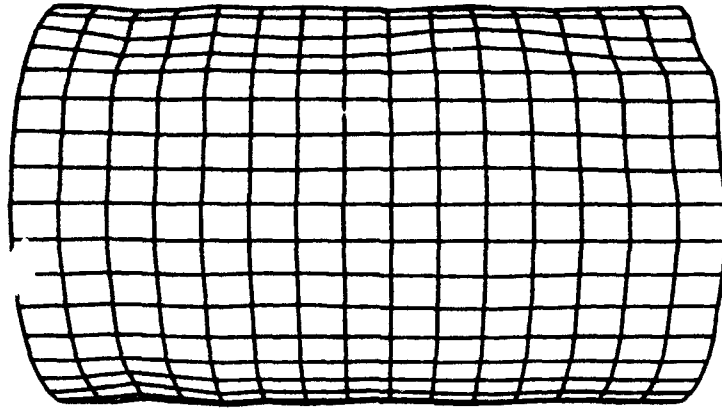
Figure 39. Deformation of Three Dimensional Ring Stiffened Finite Length Cylinder Subjected to a Square Pressure Pulse of 500 psi for 1ms

Shock →
Wave



End View $A_s = 0.0001h$

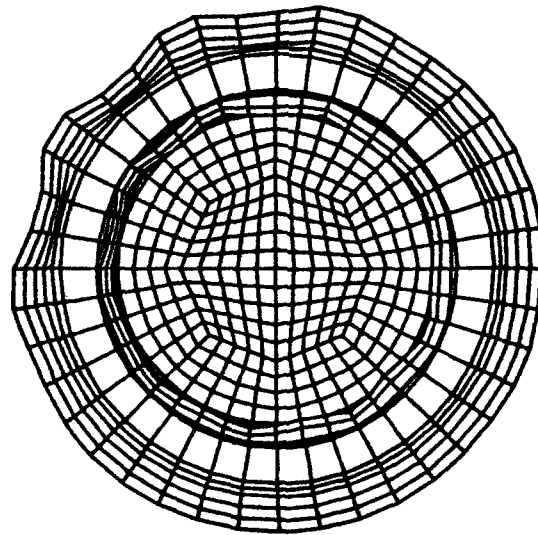
Figure 40. Deformation of Three Dimensional Ring Stiffened Finite Length Cylinder Subjected to a Square Pressure Pulse of 500 psi for 1ms



Front View $A_s = 0.0005h$

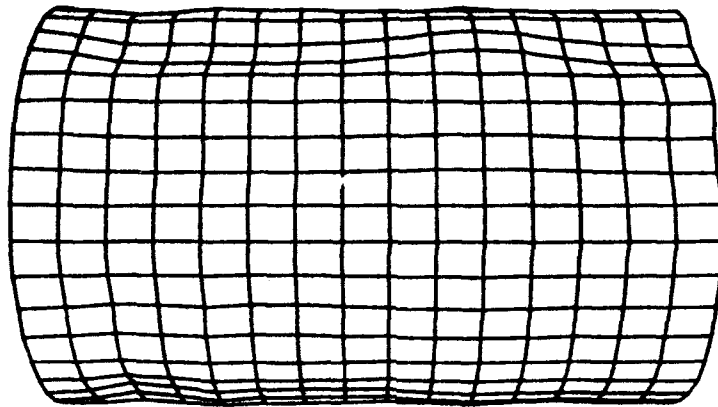
Figure 41. Deformation of Three Dimensional Ring Stiffened Finite Length Cylinder Subjected to a Square Pressure Pulse of 500 psi for 1ms

Shock→
Wave



End View $A_s = 0.0005h$

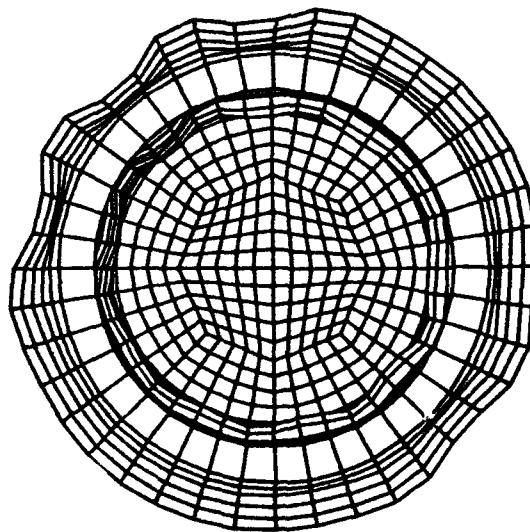
Figure 42. Deformation of Three Dimensional Ring Stiffened Finite Length Cylinder Subjected to a Square Pressure Pulse of 500 psi for 1ms



Front View $A_s = 0.001h$

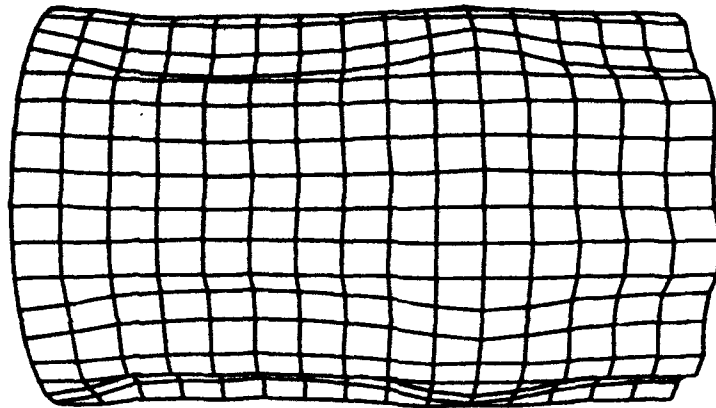
Figure 43. Three Dimensional Ring Stiffened Finite Length Cylinder Subjected to a Square Pressure Pulse of 500 psi for 1ms Deformations at 5 milliseconds

Shock →
Wave



End View $A_s = 0.001h$

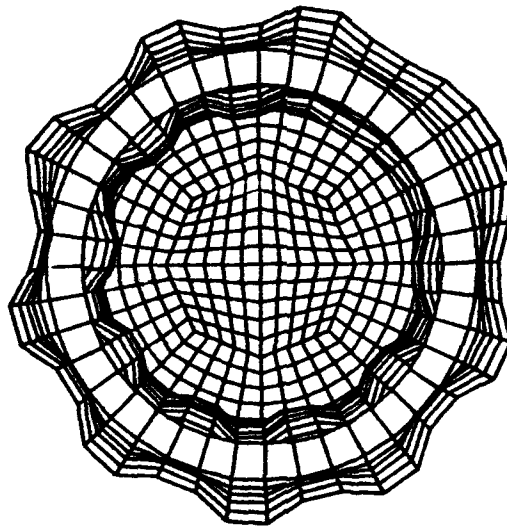
Figure 44. Three Dimensional Ring Stiffened Finite Length Cylinder Subjected to a Square Pressure Pulse of 500 psi for 1ms Deformations at 5 milliseconds



Front View $A_r = 0.005h$

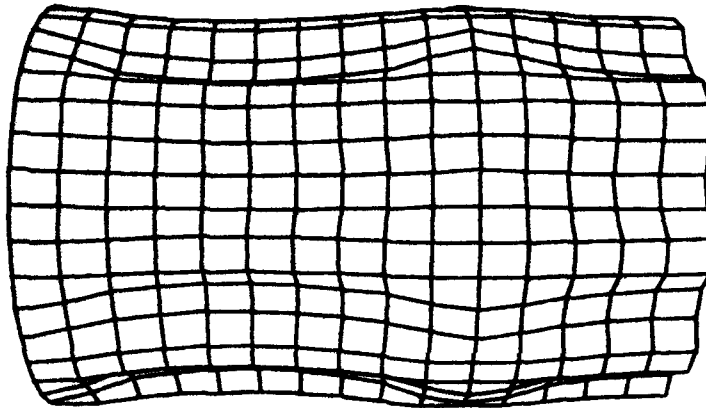
Figure 45. Three Dimensional Ring Stiffened Finite Length Cylinder Subjected to a Square Pressure Pulse of 500 psi for 1ms Deformations at 5 milliseconds

Shock→
Wave



End View $A_r = 0.005h$

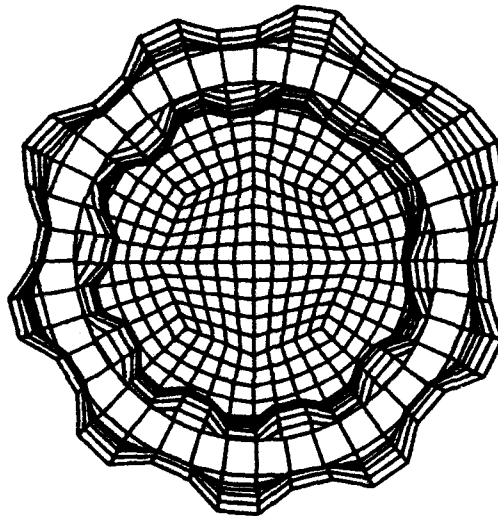
Figure 46. Three Dimensional Ring Stiffened Finite Length Cylinder Subjected to a Square Pressure Pulse of 500 psi for 1ms Deformations at 5 milliseconds



Front View $A_s = 0.01h$

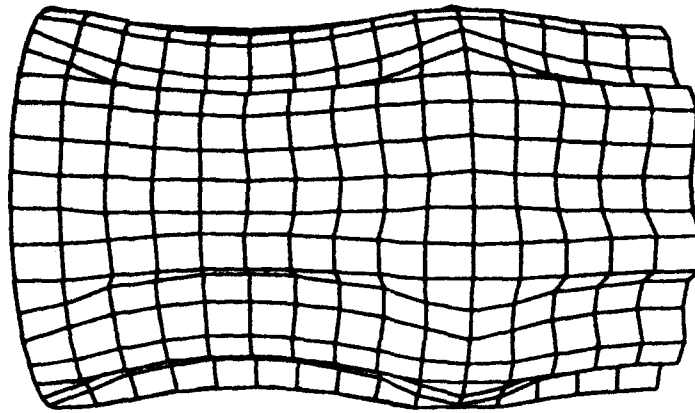
Figure 47. Three Dimensional Ring Stiffened Finite Length Cylinder Subjected to a Square Pressure Pulse of 500 psi for 1ms Deformations at 5 milliseconds

Shock→
Wave



End View $A_s = 0.01h$

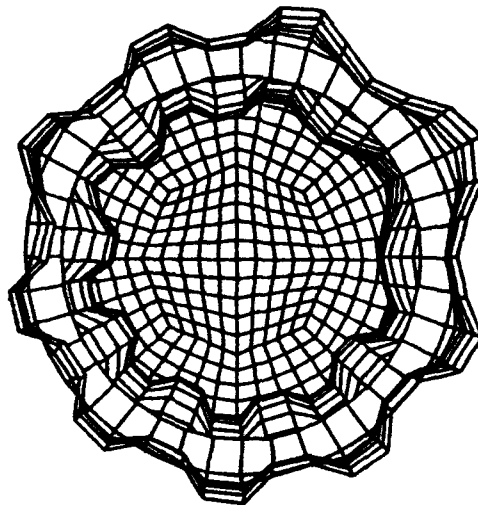
Figure 48. Three Dimensional Ring Stiffened Finite Length Cylinder Subjected to a Square Pressure Pulse of 500 psi for 1ms Deformations at 5 milliseconds



Front View $A_s = 0.05h$

Figure 49. Three Dimensional Ring Stiffened Finite Length Cylinder Subjected to a Square Pressure Pulse of 500 psi for 1ms Deformations at 5 milliseconds

Shock →
Wave



End View $A_s = 0.05h$

Figure 50. Three Dimensional Ring Stiffened Finite Length Cylinder Subjected to a Square Pressure Pulse of 500 psi for 1ms Deformations at 5 milliseconds

imperfection has changed from the pattern for the perfect cylinder. At a modal amplitude of 0.05% this alteration of the pattern is quite obvious. The pinching of the shell of the cylinder persists until higher modal amplitudes are reached. Finally at a modal amplitude of 0.5 % the pinching of the shell is eliminated. It should be noted that an amplitude of 0.5% of the shell thickness represents a modal amplitude of 0.0003 inches for this model. This magnitude of imperfections would almost certainly be present in a test cylinder.

The development of a raised section on the cylinder facing the shock wave was unexpected. With the previous perfect cylinder the shock wave impacted the cylinder along the line of nodes at the front of the cylinder. The cylinder was then rotated so that the shock wave would impact the cylinder along a line of elements. The resulting deformation pattern is shown in Figure 51. There is still a local raised section on the cylinder facing the shock wave direction. Thus, it is felt that the shot geometry of the finite element mesh is not a contributing factor to the development of this raised section.

In addition, a very specific imperfection was introduced in the five nodes facing the explosive charge centrally located in the midbay of the cylinder. This imperfection was an inward imperfection of the node

Shock→
Wave

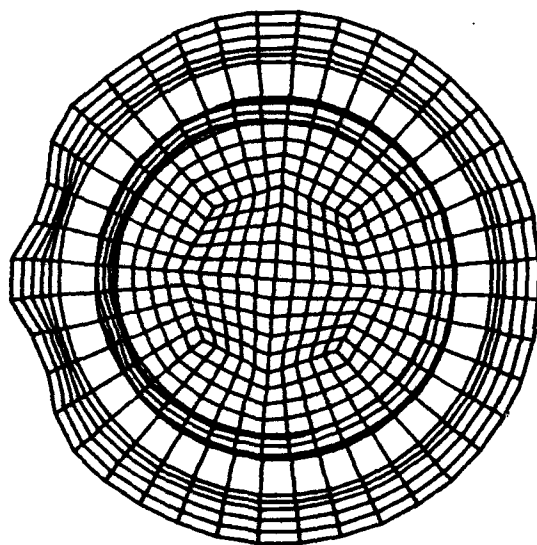


Figure 51. Three Dimensional Ring Stiffened Finite Length
Cylinder Subjected to a Square Pressure Pulse of 500 psi for
1ms Cylinder Rotated 4.5 Degrees End View Final Deformation
at 5 milliseconds

locations with an amplitude of 1% of the shell thickness (0.006 inches). The damage pattern resulting from a 500 psi 1 millisecond shock wave is shown in Figure 52.

The use of Hughes-Liu shell element (Hughes 1981) vice the Belytschko-Tsay shell element was investigated. The Hughes-Liu shell element does not use many of the simplifying assumptions used in formulating the Belytschko-Tsay shell element. As a result, the use of the Hughes-Liu shell element requires longer computational times that may not be acceptable in certain models. Figures 53 and 54 show the resulting deformation to a model using Hughes-Liu shell elements. This model is identical to the previous models with the exception of the use of the Hughes-Liu shell element. This model has initial imperfections with the first 10 modes and modal amplitudes of 1% of the shell thickness and random phase shifts. Comparison of Figures 53 and 54 with Figures 47 and 48 shows that the Hughes-Liu and the Belytschko-Tsay shell elements have the same final deformations. In this case the use of the numerically more complicated Hughes-Liu shell element is not warranted.

C. Exponential Decay Shock Wave

The use of an explosive shock wave modeled as a square wave is representative of a very large explosion at a great standoff distance from the cylinder. In order to model a

Shock→
Wave

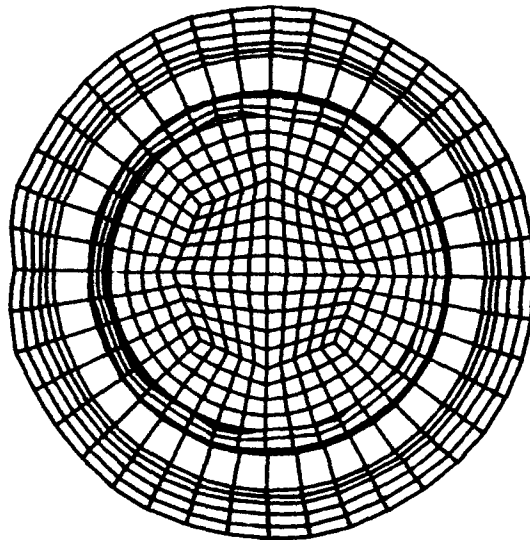
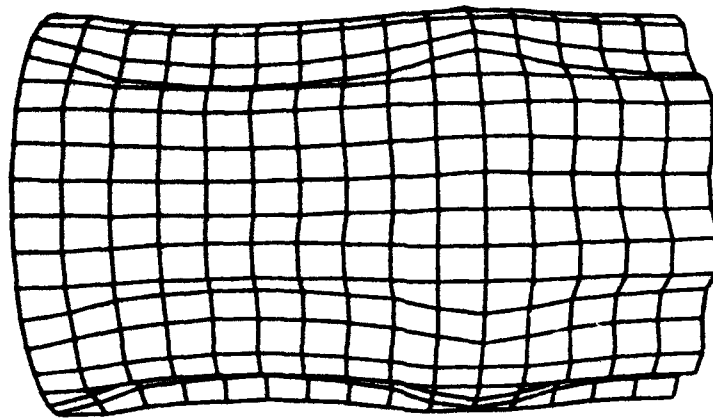


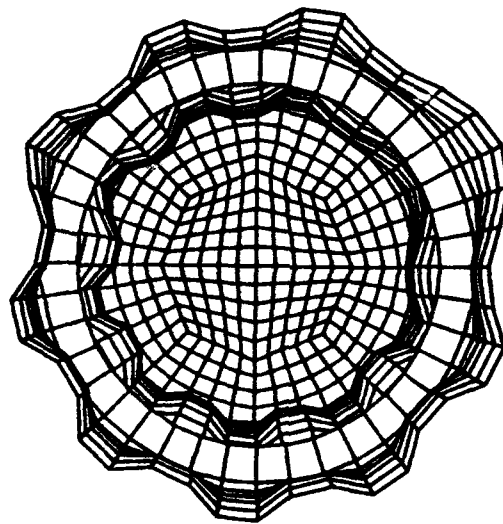
Figure 52. Three Dimensional Finite Cylinder Subjected to a Square Pressure Pulse of 500 psi 1ms End View Initial Imperfection Front Midbay Nodes 1% Offset Radially Inward Final Deformation at 5 milliseconds



Front View @ 5.0 ms

Figure 53. Three Dimensional Ring Stiffened Finite Length Cylinder Hughes-Liu Shell Elements Subjected to a Square Pressure Pulse of 500 psi for 1 ms Initial Imperfection First 10 Modes $A_n = 0.01h$ with Random Phase Shift Final Deformation at 5 milliseconds

Shock →
Wave

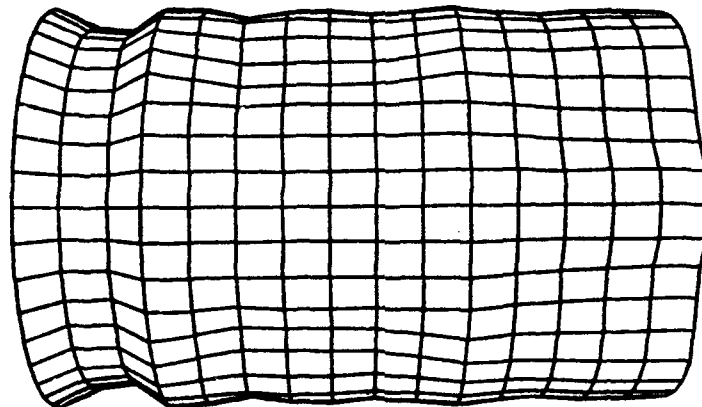


End View @ 5.0 ms

Figure 54. Three Dimensional Ring Stiffened Finite Length Cylinder Hughes-Liu Shell Elements Subjected to a Square Pressure Pulse of 500 psi for 1 ms Initial Imperfection First 10 Modes $A_n = 0.01h$ with Random Phase Shift Final Deformation at 5 milliseconds

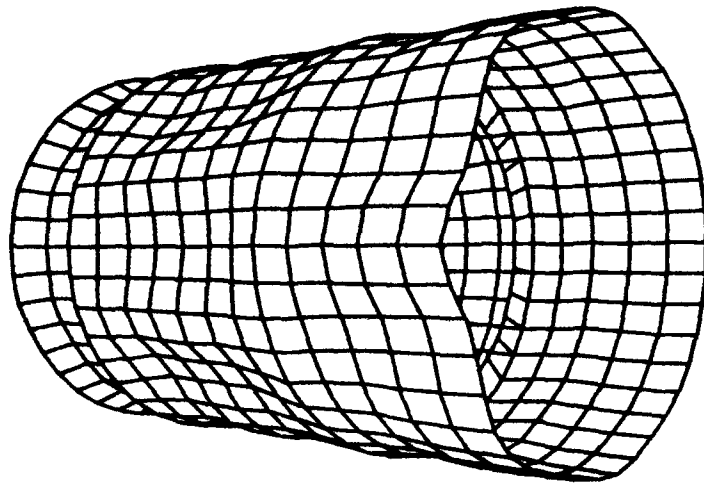
smaller explosion close to the cylinder a pressure profile corresponding to that produced by 40 pounds of PETN at a standoff distance of 30 feet was used. This explosion produces a peak pressure of 1839 psi and an exponentially decaying pressure history with a time constant of 0.377 milliseconds. The resulting damage to the cylinder from this shock wave is shown in Figure 55 through 57. From the offset view it can be seen that the response of the cylinder is different from that to the previous plane wave. The small standoff distance causes the shock wave to be a spherical wave at the cylinder. The midbay still has a protrusion of the shell material toward the explosive charge however the endbay shell material has a depression of the shell facing the charge. Also evident from the front view is the severe pinching of the shell near the endplate and on either side of the stiffener. This pinching was very severe near the endplate.

The introduction of a 5% mode 6 imperfection to the model (Figure 58) results in the deformations shown in Figure 59 and 60. Again, it is evident that the damage pattern of the cylinder due to the explosive shock clearly followed the initial imperfection. The pinching of the shell material near the endplate and stiffeners was reduced but not eliminated.



Front View

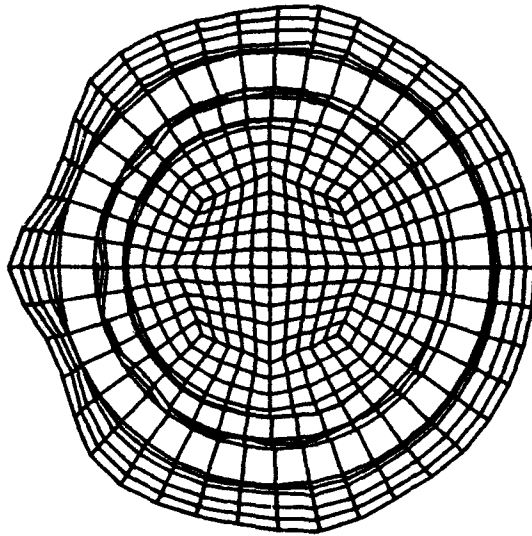
Figure 55. Three Dimensional Ring Stiffened Finite Length
Cylinder Subjected to a Pressure Pulse from 40 lbs PETN 30
Foot Standoff Final Deformation at 5 milliseconds



Offset View

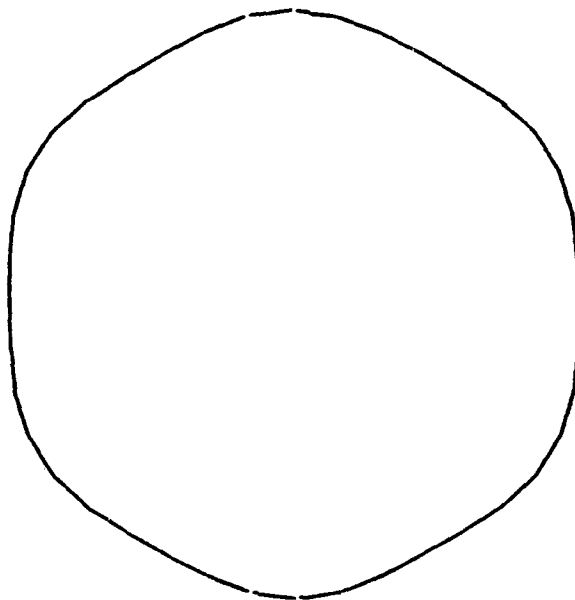
Figure 56. Three Dimensional Ring Stiffened Finite Length Cylinder Subjected to a Pressure Pulse from 40 lbs PETN 30 Foot Standoff Final Deformation at 5 milliseconds

Shock→
Wave



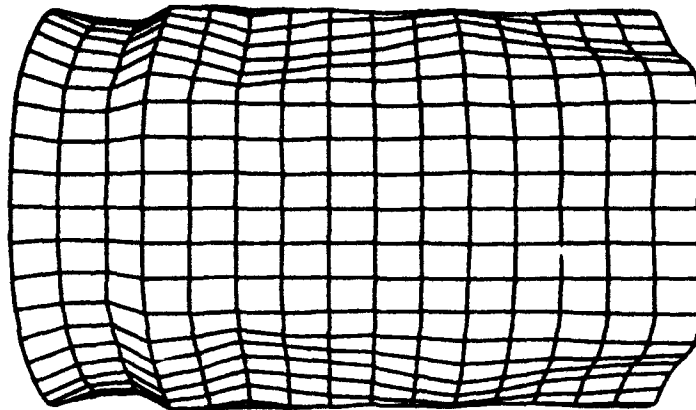
End View

Figure 57. Three Dimensional Ring Stiffened Finite Length Cylinder Subjected to a Pressure Pulse from 40 lbs PETN 30 Foot Standoff Final Deformation at 5 milliseconds



Initial Imperfection (imperfections scaled up 100X)

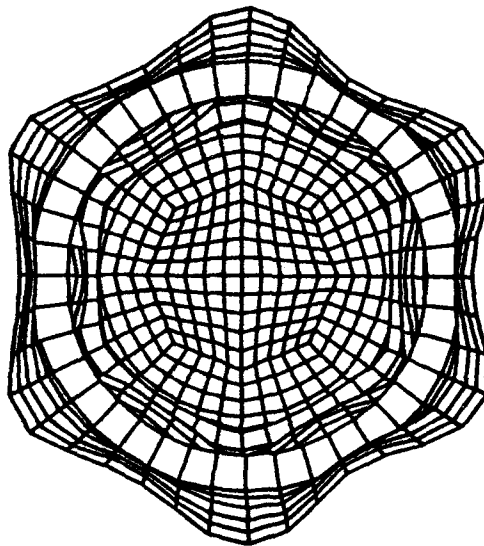
Figure 58. Three Dimensional Ring Stiffened Finite Length
Cylinder Subjected to a Pressure Pulse from 40 lbs PETN 30
Foot Standoff Initial Mode 6 Imperfection $A_6 = 0.05h$



Front View @ 5.0 ms

Figure 59. Three Dimensional Ring Stiffened Finite Length Cylinder Subjected to a Pressure Pulse from 40 lbs PETN 30 Foot Standoff Initial Mode 6 Imperfection $A_6=0.05h$

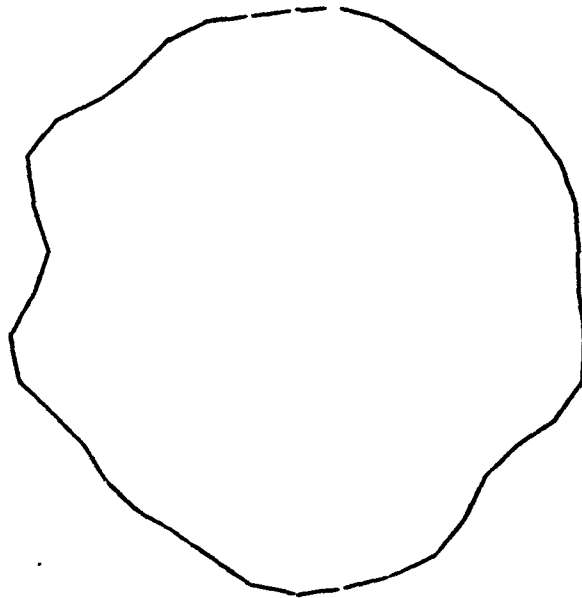
Shock→
Wave



End View @ 5.0 ms

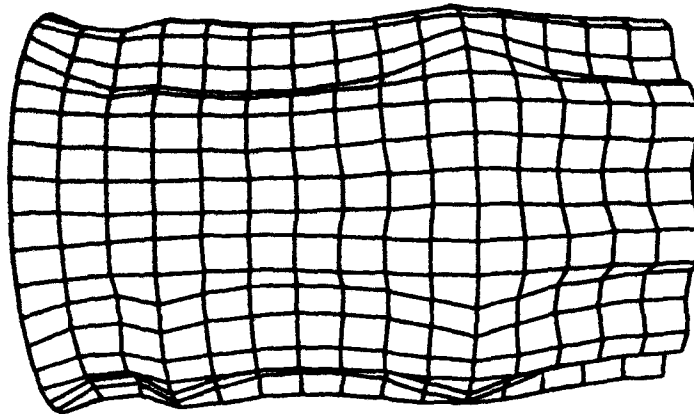
Figure 60. Three Dimensional Ring Stiffened Finite Length Cylinder Subjected to a Pressure Pulse from 40 lbs PETN 30 Foot Standoff Initial Mode 6 Imperfection $A_6=0.05h$

Introducing an imperfection of the first 10 mode shapes with a modal amplitude of 1% of the shell thickness with random phase shifts (Figure 61) results in the final damage pattern shown in Figure 62 and 63. The deformation of the shell of the cylinder was again influenced by the initial imperfection pattern. The local pinching of the shell material on either side of the stiffener was eliminated and the pinching near the endplate was reduced in magnitude.



Initial Imperfection (imperfections scaled up 200X)

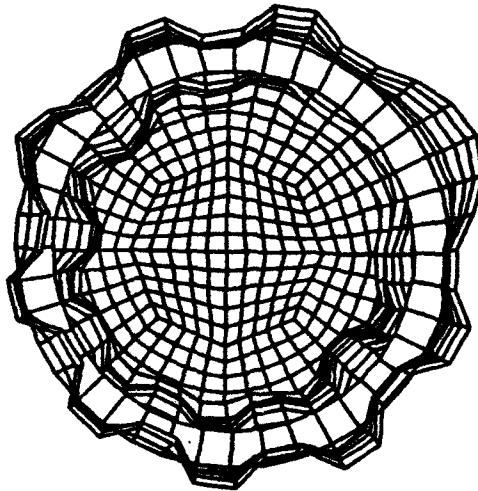
Figure 61. Three Dimensional Ring Stiffened Finite Length Cylinder Subjected to a Pressure Pulse from 40 lbs PETN 30 Foot Standoff Initial Imperfection First 10 modes $A_n = 0.01h$ with Random Phase Shift



Front View @ 5.0 ms

Figure 62. Three Dimensional Ring Stiffened Finite Length Cylinder Subjected to a Pressure Pulse from 40 lbs PETN 30 Foot Standoff Initial Imperfection First 10 modes $A_n = 0.01h$ with Random Phase Shift

Shock →
Wave



End View @ 5.0 ms

Figure 63. Three Dimensional Ring Stiffened Finite Length Cylinder Subjected to a Pressure Pulse from 40 lbs PETN 30 Foot Standoff Initial Imperfection First 10 modes $A_n = 0.01h$ with Random Phase Shift

VI. SUMMARY AND CONCLUSIONS

The response of test cylinders to underwater explosive shock is a complicated function of many factors. One important factor that is often overlooked in the modeling of these underwater shock phenomena is the initial imperfections that are present in the test cylinders. The response of model cylinders subjected to simulated underwater explosive shock has been shown to be very dependent to the initial imperfections introduced into the cylinder models. The introduction of these imperfections not only caused the shape of the shell of the cylinder (as viewed from the end) to follow the shape of the initial imperfection but it has also changed the response of the shell near the endplates and stiffeners of the model cylinder. The pinching of the shell near these stiffeners and endplates was greatly reduced or eliminated by the introduction of initial imperfections in the model cylinders. This resulting response is closer to the response observed in test cylinders subjected to actual underwater shock loading. In addition, the initial imperfections introduced increased the magnitude of the shell deformations compared to the deformations for cylinders modeled as perfect cylinders. If the initial imperfections of a test cylinder are known and introduced

into a model cylinder used in finite element analysis, the results of the finite element analysis may simulate the actual response of the test cylinder more closely.

REFERENCES

- Arbocz, J. (1982). "The Imperfection Data Bank, A Means to Obtain Realistic Buckling Loads." In *Buckling of Shells, Proc. of a State-of-the-Art Colloquium*, New York, N.Y.
- Belytschko, T. B. and Tsay, C. S. (1984). "Explicit Algorithms for Nonlinear Dynamics of Shells." *Comp. Meth. Appl. Mech. Eng.*, 43, pp. 21-276.
- Chisum, J. E. (1992). *Response Predictions for Double Hull Cylinders Subjected to Underwater Shock Loading*. Engineer's Thesis, Naval Postgraduate School, Monterey, CA.
- Fox, P. K. (1992) *Nonlinear Dynamic Response of Cylindrical Shells Subjected to Underwater Side-on Explosions*. Master's Thesis, Naval Postgraduate School, Monterey CA.
- Hallquist, J. O., and Stillman, D. W. (1990). "VEC/DYNA3D Users Manual (Nonlinear Dynamic Analysis of Structures in Three Dimensions)." Livermore Software Technology Corporation Report 1018.
- Hughes, T. J. R., Liu, W. K., and Levitt, I., (1981). "Nonlinear Dynamics Finite Element Analysis of Shells." *Nonlinear Finite Element Analysis in Struct. Mech.*, Eds. W. Wunderlich, E. Stein and K. J. Bathe, Springer-Verlag, Berlin, pp. 151-168.
- Kirkpatrick, S. W., and Holmes, B. S. (1989). "Effect of Initial Imperfections on Dynamic Buckling of Shells." *Journal of Engineering Mechanics*, v. 115, pp. 1075-1093.
- Lindeberg, H. E., and Florence, A. L. (1987). *Dynamic Pulse Buckling*. Martinus Nijhoff Publishers, Dordrecht, The Netherlands.

APPENDIX A

INGRID INPUT FILE FOR TWO DIMENSIONAL INFINITE CYLINDER
MODEL

INFINITE CYLINDER MODEL

dn3d vec term 5.0e-3 plti 1.0e-5 prti 1000.

mat 1 type 3 e 2.9e+7 pr 0.3 ro 7.356e-4
etan 5.1e+4 sigy 3.2e+4 shell quad 5 thick 0.060 endmat

lcd 1 2 0.0 0.0 1.0 0.0
lcd 2 2 0.0 2.5e-8 1.0 2.5e-8

plan 2

0 0 -.003 0 0 -1 0.001 symm
0 0 .003 0 0 1 0.001 symm

start

-1 6 -11 ;
-1 6 -11 ;
1 2 ;
-1. 0. 1.
-1. 0. 1.
-.003 .003
a 1 1 0 3 3 0 3 6.0
pri -1 -3 ; -1 -3 ; ; 1 -1.0 0. 0. 0.
mate 1
end
end

APPENDIX B

INGRID INPUT FILE FOR THREE DIMENSIONAL STIFFENED INFINITE CYLINDER MODEL

STIFFENED INFINITE CYLINDER MODEL

dn3d vec term 5.0e-3 plti 1.0e-5 prti 1000.

c

c material definitions

c

c shell material (mild steel)

c

mat 1 type 3 e 2.9e+7 pr 0.3 ro 7.356e-4
etan 5.1e+4 sigy 3.2e+4 shell quad 5 thick 0.060 endmat

c

c stiffener material (mild steel)

c

mat 2 type 3 e 2.9e+7 pr 0.3 ro 7.356e-4
etan 5.1e+4 sigy 3.2e+4 shell quad 5 thick 0.12 endmat

c

c load curve definitions

c

lcd 1 2 0.0 0.0 1.0 0.0
lcd 2 2 0.0 1.0e-6 1.0 1.0e-6

c

c symmetry planes

c

plan 2

0 0 -6. 0 0 -1 0.001 symm
0 0 6. 0 0 1 0.001 symm

c

c construct shell

c

start

-1 11 -21 ;
-1 11 -21 ;
1 6 11 ;
-1. 0. 1.
-1. 0. 1.
-6. 0. 6.

```
a 1 1 0 3 3 0 3 6.0
pri -1 -3 ; -1 -3 ; ; 1 -1.0 0. 0. 0.
mate 1
end
c
c    construct stiffener
c

start

1 2 12 22 23 ;
1 2 12 22 23 ;
-1 ;
-1 -1 0 1 1
-1 -1 0 1 1
0
di 1 2 0 4 5 ; 1 2 0 4 5 ; ;
a 1 1 0 5 5 0 3 6.0
a 2 2 0 4 4 0 3 5.0
d 2 2 0 4 4 0
mate 2
end
end
```

APPENDIX C

INGRID INPUT FILE FOR THREE DIMENSIONAL STIFFENED FINITE CYLINDER MODEL

STIFFENED FINITE CYLINDER

dn3d vec term 5.0e-3 plti 1.0e-5 prti 1000.

C

C material definitions

C

C shell material (mild steel)

C

mat 1 type 3 e 2.9e+7 pr 0.3 ro 7.356e-4
etan 5.1e+4 sigy 3.2e+4 shell quad 5 thick 0.060 endmat

C

C stiffener material (mild steel)

C

mat 2 type 3 e 2.9e+7 pr 0.3 ro 7.356e-4
etan 5.1e+4 sigy 3.2e+4 shell quad 5 thick 0.12 endmat

C

C endplate material (HY-100 steel)

C

mat 3 type 3 e 2.9e+7 pr 0.3 ro 7.356e-4
etan 5.02e+4 sigy 1.08e+5 shell quad 5 thick 0.25

endmat

C

C load curve definitions

C

lcd 1 2 0.0 0.0 1.0 0.0
lcd 2 2 0.0 1.0e-6 1.0 1.0e-6

C

C symmetry planes

C

plan 1

0 0 0.0 0 0 -1 0.001 symm

C

C construct shell

C

```

start
-1 6 -11 ;
-1 6 -11 ;
 1 16 ;
-1. 0. 1.
-1. 0. 1.
 0.0 18.0
a 1 1 0 3 3 0 3 6.0
pri -1 -3 ; -1 -3 ; ; 1 -1.0 0. 0. 0.
mate 1
end

```

```

c
c   construct stiffener
c

```

```

start
1 2 7 12 13 ;
1 2 7 12 13 ;
-1 ;
-1 -1 0 1 1
-1 -1 0 1 1
6.0
di 1 2 0 4 5 ; 1 2 0 4 5 ; ;
a 1 1 0 5 5 0 3 6.0
a 2 2 0 4 4 0 3 5.0
d 2 2 0 4 4 0
mate 2
end

```

```

c
c   construct endplate
c
c   surface definitions
c
sd 1 cyli 0 0 0 0 0 1 6.0
sd 2 cyli 0 0 0 0 0 1 [6.0*3/5]

```

```

start
 1 5 10 15 19 ;
 1 5 10 15 19 ;
-1 ;
-1 -1 0 1 1
-1 -1 0 1 1
18.0
pr 1 1 1 5 5 1 1 -1.0 0.0 0.0 0.0
di 1 2 0 4 5 ; 1 2 0 4 5 ; ;
sfvi -2 -4 ; -2 -4 ; ; sd 2
sfi -1 -5 ; -1 -5 ; ; sd 1
mate 3

```

end
end

APPENDIX D

FORTRAN PROGRAMS FOR MODIFYING INGRIDO FILE FOR MODAL IMPERFECTIONS

```

program imp
*****
* This program written by Donald T. Hooker II on 3/15/93 *
* Revised 5/12/93 *
*****
* This program modifies the nodes of a file called *
* "ingrido.raw", which is an edited version of ingrido in *
* which the first line is the beginning of the node list. *
* This is one of a series of 2 programs, which need to be *
* run in order, i.e. "imp" then "convert". These programs *
* modify the node positions for modal imperfections WITH *
* OR WITHOUT random amplitudes and/or phase shifts. The *
* final output file name is imp.dat. *
*****
* VARIABLE DECLARATION *
* a - angle from reference axis to radial position of *
* node *
* a1 thru a10 - weighting factor for each modal *
* imperfection *
* b1 - ingrido constants *
* b2 - ingrido constants *
* dr - change in radial position due to modal *
* imperfections *
* dr1 thru dr10 - radial position change for each modal *
* imperfection *
* h - thickness of shell *
* n - node number *
* m - number of nodes *
* pi - 3.14159265359 *
* ps1 thru ps10 - phase shift for each modal *
* imperfection *
* r - radial position of node *
* randamp - if random amplitude is desired set randamp=1 *
* randphs - if random phase is desired set randphs=1 *
* x - x coordinate of node *
* y - y coordinate of node *
* z - z coordinate of node *
*****

double precision x,y,z,a,r,dr,h,pi
double precision a1,a2,a3,a4,a5,a6,a7,a8,a9,a10
double precision dr1,dr2,dr3,dr4,dr5,dr6,dr7,dr8,dr9,
& dr10
double precision ps1,ps2,ps3,ps4,ps5,ps6,ps7,ps8,ps9,
& ps10

```

integer randamp, randphs

```
*****  
*   OPEN INPUT AND OUTPUT FILES   *  
*****
```

```
open(14,file='ingrido.raw')  
open(15,file='imp.unconverted')
```

```
*****  
*   IF RANDOM MODE AMPLITUDE IS DESIRED SET RANDAMP EQUAL *  
*   TO 1   *  
*   IF RANDOM MODE PHASE SHIFT IS DESIRED SET RANDPHS   *  
*   EQUAL TO 1   *  
*****
```

```
randamp = 0  
randphs = 1
```

```
*****  
*   INPUT NUMBER OF NODES TO BE MODIFIED AND WRITE NUMBER *  
*   TO OUTPUT FILE IMP.UNCONVERTED   *  
*****
```

```
m = 921  
write(15,98)m  
98 format(1x,i5)
```

```
*****  
*   INPUT THICKNESS OF SHELL   *  
*****
```

```
h = 0.06
```

```
*****  
*   SET THE VALUE OF PI   *  
*****
```

```
pi = 3.14159265359
```

```
*****  
*   INPUT THE WEIGHTING COEFFICIENTS OF THE FIRST TEN   *  
*   MODE SHAPES   *  
*****
```

```
a1 = 0.01  
a2 = 0.01  
a3 = 0.01  
a4 = 0.01  
a5 = 0.01  
a6 = 0.01
```

```
a7 = 0.49
a8 = 0.64
a9 = 0.81
a10 = 1.0
```

```
*****
* INPUT PHASE SHIFT FOR EACH MODE SHAPE *
```

```
ps1 = 0.0
ps2 = 0.0
ps3 = 0.0
ps4 = 0.0
ps5 = 0.0
ps6 = 0.0
ps7 = 0.0
ps8 = 0.0
ps9 = 0.0
ps10 = 0.0
```

```
*****
* INPUT SEED NUMBER FOR RANDOM NUMBER GENERATOR *
```

```
seed = 1.0
```

```
*****
* CALL SUBROUTINE SRAND TO GENERATE SEED NUMBER FOR
* RANDOM NUMBER GENERATOR SUBROUTINE *
```

```
call srand(seed)
```

```
*****
* CALL SUBROUTINE RAND TO GENERATE RANDOM PHASE SHIFT
* FOR EACH MODE SHAPE *
```

```
if (randpms .eq.1) then
  ps1 = 2. * pi * rand()
  ps2 = 2. * pi * rand()
  ps3 = 2. * pi * rand()
  ps4 = 2. * pi * rand()
  ps5 = 2. * pi * rand()
  ps6 = 2. * pi * rand()
  ps7 = 2. * pi * rand()
  ps8 = 2. * pi * rand()
  ps9 = 2. * pi * rand()
  ps10 = 2. * pi * rand()
endif
```

```
*****
```

```

* CALL SUBROUTINE RAND TO GENERATE RANDOM WEIGHTING OF *
* MODE SHAPES *
*****

```

```

if (randamp .eq. 1) then
  a1 = a1 * rand()
  a2 = a2 * rand()
  a3 = a3 * rand()
  a4 = a4 * rand()
  a5 = a5 * rand()
  a6 = a6 * rand()
  a7 = a7 * rand()
  a8 = a8 * rand()
  a9 = a9 * rand()
  a10 = a10 * rand()
endif

```

```

*****
* DO LOOP TO READ INPUT DATA *
*****

```

```

do 100 i=1,m
  read(14,*) n,b1,x,y,z,b2

```

```

*****
* CALCULATE RADIUS OF NODE POSITION *
* (Look carefully at the axis of rotation of the *
* cylinder to determine the proper cartesian *
* coordinates used to calculate the radius of the *
* cylinder. In this case the axis of rotation is the z *
* axis. *
*****

```

```

r=(x*x+y*y)**0.5

```

```

*****
* CALCULATE THE ANGLE FROM THE REFERENCE AXIS TO THE *
* NODE POINTS (Look carefully at the zero angle *
* direction. In this case the x axis points in the *
* direction of the charge.) *
*****

```

```

if ((dabs(y).lt. 0.001)) then
  if (x.gt.0.0) then
    a=0.0
  else
    a=pi
  endif
else
  a=datan(y/x)
  if (x.lt.0.0) then

```

```
      a=a+pi
    endif
  endif
```

```
*****
*   MODIFY THE NODE POSITIONS USING THE FIRST TEN MODE   *
*   SHAPES                                               *
*****
```

```
      dr1 = a1 * h * dcos(a + ps1)
      dr2 = a2 * h * dcos(2. * a + ps2)
      dr3 = a3 * h * dcos(3. * a + ps3)
      dr4 = a4 * h * dcos(4. * a + ps4)
      dr5 = a5 * h * dcos(5. * a + ps5)
      dr6 = a6 * h * dcos(6. * a + ps6)
      dr7 = a7 * h / 7. / 7. * dcos(7. * a + ps7)
      dr8 = a8 * h / 8. / 8. * dcos(8. * a + ps8)
      dr9 = a9 * h / 9. / 9. * dcos(9. * a + ps9)
      dr10 = a10 * h / 10. / 10. * dcos(10 * a + ps10)
      dr = dr1 + dr2 + dr3 + dr4 + dr5 + dr6 + dr7 + dr8 +
&      dr9 + dr10
```

```
*****
*   CALCULATE THE CARTESIAN COORDINATES OF THE NODES   *
*****
```

```
      x=x-dr*dcos(a)
      y=y-dr*dsin(a)
```

```
*****
*   WRITE DATA TO TEMPORARY DATA FILE IMP.UNCONVERTED *
*****
```

```
      write(15,998) n,b1,x,y,z,b2
998   format(i8,f5.0,3e20.13,f5.0)
100   continue
```

```
*****
*   CLOSE INPUT AND OUTPUT FILES                       *
*****
```

```
      close(14)
      close(15)
      stop
      end
```

program convertimp

```
*****
*   This program written by Donald T. Hooker II on 3/15/93   *
*   Revised 3/30/93                                           *
*****
*   This program converts numerical data
from'imp.unconverted'*
*   into ascii format for use in modifying ingrido for modal*
*   imperfections                                             *
*****
*   VARIABLE DECLARATION                                       *
*   f* - data to be converted to ascii format                 *
*   m - number of nodes                                       *
*****

character*13 f1
character*1 f2,f3,fz
character*18 f4
character*1 f5,f6
character*18 f7
character*1 f8,f9
character*18 f10
character*5 f11
open(14,file='imp.unconverted')
open(15,file='imp.dat')
fz='0'

*****
*   READ NUMBER OF NODES TO BE MODIFIED                       *
*****

read(14,*) m

*****
*   DO LOOP TO READ DATA AND CONVERT IT TO ASCII FORMAT     *
*****

do 100 i=1,m
  read(14,998)f1,f2,f3,f4,f5,f6,f7,f8,f9,f10,f11
998  format(a13,a1,a1,a18,a1,a1,a18,a1,a1,a18,a5)
  write(15,998)f1,f3,fz,f4,f6,fz,f7,f9,fz,f10,f11
100 continue

*****
*   CLOSE INPUT AND OUTPUT FILES                               *
*****

close(14)
close(15)
stop
```

end

INITIAL DISTRIBUTION LIST

	No. of Copies
1. Defense Technology Information Center Cameron Station Alexandria, Virginia 22304-6145	2
2. Library, Code 52 Naval Postgraduate School Monterey, California 93943-5002	2
3. Professor Y. S. Shin, Code ME/Sg Department of Mechanical Engineering Naval Postgraduate School Monterey, California 93943	2
4. Professor Y. W. Kwon, Code ME/Kw Department of Mechanical Engineering Naval Postgraduate School Monterey, California 93943	2
5. Dr. Kent Goering Defense Nuclear Agency 6801 Telegraph Road Alexandria, Virginia 22310	1
6. Mr. Douglas Bruder Defense Nuclear Agency 6801 Telegraph Road Alexandria, Virginia 22310	1
7. Dr. Roshdy S. Barsoum Office of Naval Research Mechanics Division, Code 1132 800 North Quincy Street Arlington, Virginia 22217-5000	1
8. LT Michael P. Rousseau, USN 735 Lily Street Monterey, California 93940	1
9. LT Donald T. Hooker II, USN 378 F Bergin Drive Monterey, California 93940	1